On Impact Dynamics of Robotic Operations

Yu Wang

CMU-RI-TR-86-14

Department of Mechanical Engineering and
The Robotics Institute
Carnegie-Mellon University
Pittsburgh, Pennsylvania 15213

September 1986

Copyright ©1986 Carnegie-Mellon University

Support for this research was provided by the System Development Foundation.

Table of Contents

Abstract 1

1. Introduction 2

1.1 An Example . . . 3
1.2 Previous Work . . . 4
Impact Dynamics . . . 4
Robotic Manipulation . . . 5
1.3 Overview . . . 7

2. Background and Notation 8

2.1 Friction . . . 8
2.2 Coefficient of Restitution . . . 8
2.3 Assumptions . . . 9
2.4 Notation . . . 10

3. Analysis of Impact Process 11

3.1 Dynamic Equations of Motion . . . 11
3.2 Force Constraints . . . 12
3.2.1 Elasticity Constraint . . . 13
3.2.2 Friction Constraint . . . 13
3.3 Impact Process Diagram . . . 14
3.4 An Example . . . 17
3.5 Summary . . . 19

4. Contact Modes of Impact 21

4.1 Impact Space . . . 21
4.2 Effects of the Parameters . . . 24

5. Motions of Object after Impact 28

5.1 The Fundamental Motion . . . 28
5.2 Local Velocity at the Point of Contact . . . 29

6. Conclusion 32

Acknowledgments 33

References 34

Appendix A 36

List of Figures

Figure 1.1: An example of impact 3
Figure 1.2: The impact space diagram for the rectangular object 4
Figure 3.1: A polygonal object strikes a flat constraint surface 11
Figure 3.2: Impact process diagrams 15
Figure 3.3: All possible cases of impact process 16
Figure 3.4: The example of a sphere striking a constraint surface. 18
Figure 3.5: Motion of the sphere and the impulse 20
Figure 4.1: The three major regions of impact 21
Figure 4.2: Impact space 23
Figure 4.3: The effect of the value of r 25
Figure 4.4: The effect of the coefficient of restitution 26
Figure 4.5: Impact with very large friction 27
Figure 5.1: Changes in the rotational velocity at the point of contact 29
Figure 5.2: The locus of the translation lines for rotational velocity changes . . 30
Figure 5.3: Rebound velocity at the point of contact 31
Figure A.1: General impact of two bodies 37

ABSTRACT

For a manipulator operation, the motion of an object to be manipulated is determined by the forces applied to the object. It is important to understand the dynamics for planning successful robot operations. The presence of friction, elasticity, as well as the inertial property of the object makes the problem difficult. This paper presents an analysis of impact dynamics incorporating these phenomena. When inertial forces dominate an impact process, we find that contact modes of impact can be predicted in an impact space that represents all possible processes. The fundamental motion of the object is described by the way it will rotate. The effects of the above mentioned phenomena on the fundamental motion can be determined in the impact space. We also find that the prediction of the fundamental motion made by the quasi-static analysis is a lower bound for dynamic cases. The results of this analysis can be applied to the planning of robot manipulations. For simplicity, the operations and the object are constrained to a two dimensional space.

1. Introduction

The success or failure of any manipulation operation is determined by the physical processes involved in the operation. When objects collide during an operation, impact dynamics becomes a significant factor. For example, when a robot acquires a part, the part is inevitably subject to impact forces when the hand touches the part. When placing a part, the part is again subject to impact forces when the part collides with the bench. If these impact forces are not modeled, and if the movements of the hand are not controlled such that inappropriate forces are prevented, the robot operations may not succeed. This paper investigates the impact dynamics of the interaction of two objects. The goal of the paper is to improve our understanding of manipulation operations that involve collisions.

Uncertainty in the environment makes impact forces difficult to predict. The positions, orientations, and shapes of the parts are not known with great precision. Errors in modeling, sensing, and control produce uncertainty in the position and velocity of the robot itself. These uncertainties make it impossible to predict exactly when and where an impact will occur. Robots have to overcome not only the uncertainty but also the unpredictable impact forces to perform a successful operation.

There are several ways to overcome the problem. Most present approaches attempt to eliminate uncertainty and unpredictable effects of impact by precisely locating parts and reducing motion speeds. Another method is to use sensors to detect variations in the environment. Both strategies are slow for fine manipulation tasks.

A third method is to develop motion strategies which use the task mechanics to reduce the uncertainty without sensing. Such operations will succeed despite significant uncertainty and unpredictable forces. A planner which models inertial and impact forces could predict the behavior of an object that is subject to collisions during manipulation. The resulting operations are planned so that they are less sensitive to uncertainty and the effect of unpredictable forces.

In order to develop such successful motion strategies, it is necessary to explore manipulation operations in both static and dynamic domains. A fundamental understanding of manipulation operations that involve collisions is a first step toward the development of challenging manipulation operations, such as placing, throwing, and dynamic grasping, and to the development of better robot manipulators and manipulation systems.

In this paper we describe the impact dynamics of a rigid body striking a plane surface. For simplicity, the problem is constrained to be planar. The rigid body is assumed to be polygonal, and exhibits planar motion during impact. For generality, we assume that the surface is not perfectly elastic and is not smooth, and that the speed of the body is large enough that the impact forces dominate other forces like gravity during impact.

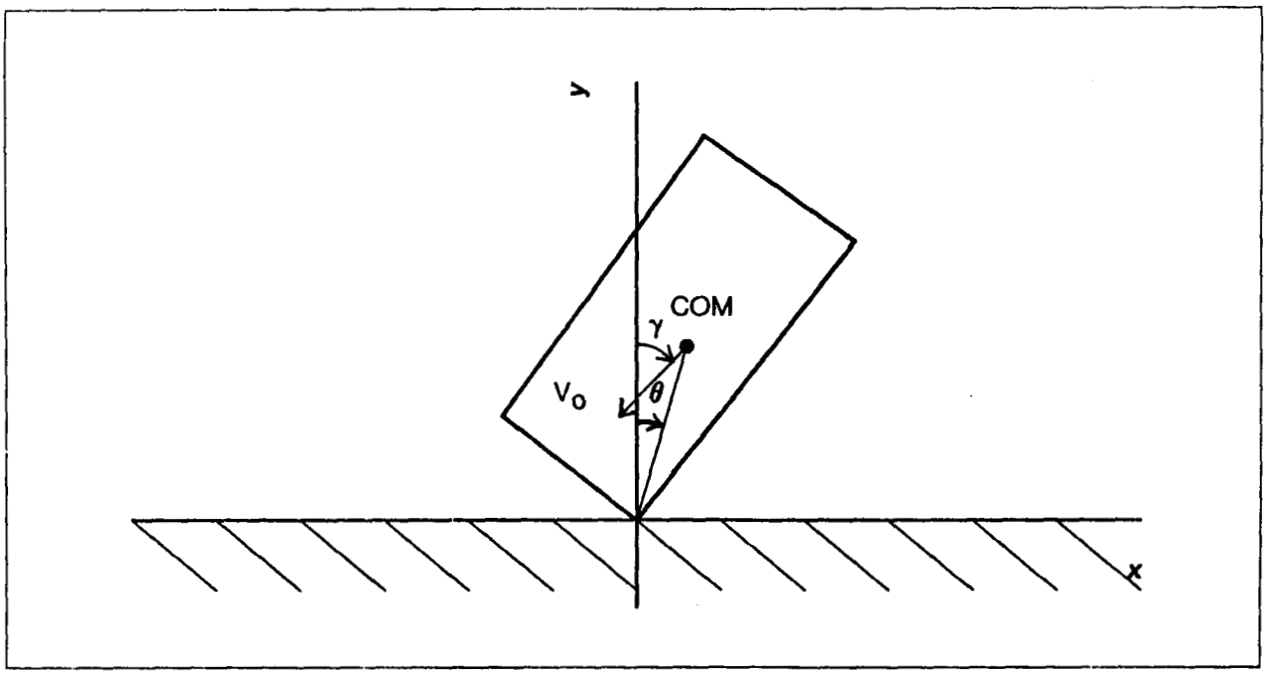


Figure 1.1. An example of impact. The rectangular object strikes the surface with an initial velocity $\mathbf{v_o}$. The object orientation and the motion direction are specified by angles θ and γ, where $\theta = 10$ degrees and $\gamma = 25$ degrees. The coefficient of friction μ is equal to 0.25, and the coefficient of restitution e is equal to 0.8. The object is 1 inch high and 2 inches long.

Within this domain, we apply a rigid body theory and present the solutions for contact mode and resulting direction of motion for all possible geometric descriptions of the process. We can determine how the motion of sliding varies its direction during the impact. The effect of inertia, friction, and elasticity to the contact mode and the motion can also be determined.

The work presented here is part of a large effort to develop automatic methods using dynamic constraints to manipulate objects. These operations include: placing an object in the hand onto a table; dynamic grasping; striking an object to make slight adjustments in the object's position; and orienting objects. Understanding and predicting the effect of impact processes is essential to the development.

1.1. An Example

We show an example in Figures 1.1 and 1.2. The object strikes the surface with initial velocity $\mathbf{v_o}$. The object orientation is represented by angle θ, and the motion direction is represented by angle γ. To make the object strike the surface, there are continua of possible object orientations and possible motion directions within certain limits. For the all possible object orientations and motion directions, possible contact modes are represented in the *impact space* shown in Figure 1.2a. In the diagram, the orientation of the object varies along the vertical axis, and the the motion direction varies along the horizontal axis.

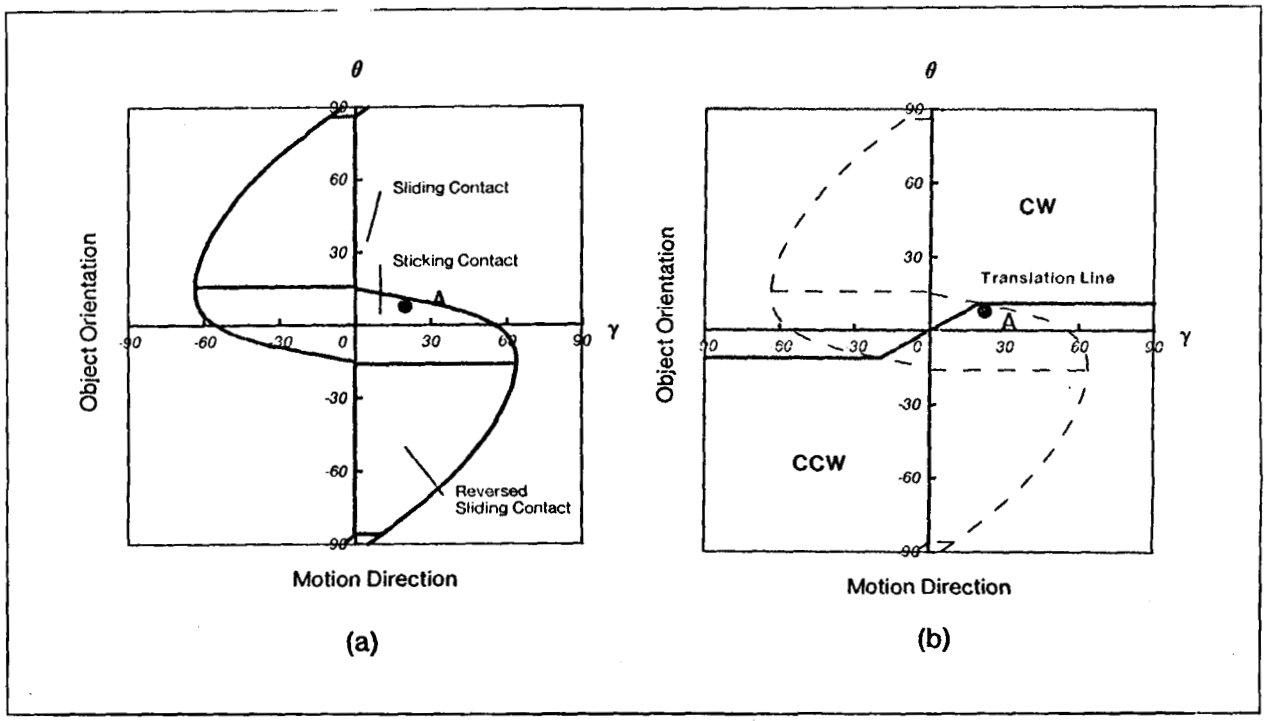


Figure 1.2. The impact space diagram for the rectangular object. The impact space is divided by the regions of variety contact modes in (a), and by the regions of clockwise and counter-clockwise rotating motions in (b).

Within this diagram, the regions shaded with solid lines indicate those impacts that the object will roll across the surface after the processes. The regions shaded with dashed lines indicate those impacts that the direction of sliding of the point of contact will undergo a reversal. Other regions correspond to the impacts that the object will slide as well as bounce.

Similarly in the impact space, Figure 1.2b shows the sense of the rotation of the object after the impact. The heavy line in the diagram corresponds to those impacts that the object only changes its translational motion, but not rotation. The regions above the line indicate that the object will rotate clockwisely, and the regions below the line indicate that the object will rotate counter-clockwisely.

The example shown in Figure 1.1 is represented by the point A in Figure 1.2. With the impact space we can predict that the object will roll across the surface with a counter-clockwise rotation.

1.2. Previous Work

Impact Dynamics

Impact phenomena have interested scientists and engineers for centuries. The initial approach to the law of impact was based on the behavior of objects as rigid bodies. Routh

studied the impact of two bodies in both planar motion and three dimensional motion [Routh 1860]. Employing the Coulomb model of friction and coefficients of restitution for energy losses, Routh derived the dynamic equations of motion after impact of the bodies. In the process of impact, the points of contact of the two bodies may slide with respect to each other, or may not. It is even possible that the relative velocity of the points in contact may reverse its direction during impact, if initially the relative velocity is not zero. Therefore, the frictional impulse during impact can not be determined by simply using Coulomb's law. To solve the problem Routh developed a graphical technique which could determine the actual changes that occur in the frictional impulse as the impact proceeds. The technique provides the basis of the work presented in this paper.

It is interesting to note that this initial approach has survived essentially unchanged to the present day and represents the only exposition of impact in most texts on dynamics [Beer and Johnston 1984; Goldsmith 1959]. During the last few decades, work on the impact problem has been concentrated on either the transient contact phenomena or the propagation of elastic and non-elastic deformations, and rarely on the modes of contact or the motions of objects subject to friction. Recently, [Maw 1976; Maw, Barber, and Fawcett 1981] extended the static approach of [Mindlin and Deresiewicz 1953] to a central contact problem of impact. The tangential compliance of the contact surface of a circular object was shown to have a significant effect on the rebound motions of the object. The Hertz theory of impact and the Coulomb model of friction were used in their analysis. By contrast, [Brach 1981] applies the rigid body theory to show the effect of the impulse moment developed between two colliding bodies. He defined a generally system-dependent coefficient of restitution to take this moment into account.

Within the framework of rigid body theory, [Keller 1986] presented a theory of the impact of two rigid bodies with friction. The main difficulty associated with his approach is the calculation of the relative tangential velocity of the point of contact. In this paper we present a geometric method that overcomes the difficulty. Furthermore, the contact modes, the impulsive forces, and the changes of motion of the bodies can be predicted in using this method.

Robotic Manipulation

In recent times, dynamic problem related to robotic manipulation have attracted much attention. For some simple manipulation operations, dynamic and impact actions must be employed. For example, in placing an object on a table, the collision of the object with the table occurs either before the release of the object from the hand, or after the release. In either case, the mechanics of the interaction between arm, object, and table determines the ultimate success of the operation.

Several authors have addressed impact forces and dynamics in automatic assembly

systems. [Drake 1977] investigated the impact dynamics of a special device for performing peg insertions at high speeds. He noted that during parts mating, the impulse forces arising from part collisions are more significant than the deflection forces that arise due to positioning errors. [Selvage 1979] examined an assembly process involving a series of impacts. The impacts become tools rather than hindrances in an efficient insertion operation. [Higuchi 1984] studied a method of micro-positioning based on the impact phenomenon. He designed a device utilizing electromagnetic impulsive forces and frictional force between an object and a supporting surface for precise positioning control. When the object is subject to electromagnetic impulsive forces and frictional forces, it can be moved microscopic distances. Using this method, a robot tool for adjusting the position and orientation of an object on a table could be developed.

In the design and construction of programmable devices for part orienting and positioning, impact problems also arise. One method of reducing the problems is careful control of materials and construction of the devices to minimize the effect of impact forces [Boothroyd 1972]. [Erdmann and Mason 1986] described an automatic planner that uses motion strategies to reduce uncertainty in the locations of parts. It is also possible to extend the planner to cover a broader model of task mechanics so that inertial forces and impact forces can be exploited.

The dynamic and impact problem is also associated with robot hand designs. The requirements for a robot hand design result from the characteristics of the object as well as the functional and structural characteristics of the hand. To develop hands which are more generic and flexible in character and performance, it is important to control and quantify the interaction between hand and object. [Parker and Paul 1984] outlined an approach of characterizing and modeling of objects and object acquisition. They proposed a method to control transient forces during object acquisition while maintaining robot-hand accuracy and precision, if the precise position of the object is known. [Hollerbach 1982] discussed mechanical problems in robot hand design and control, noting that the development of more advanced hand control strategies such as dynamic grasping is required for further study in robot control area. [Chelpanov and Kolpashnikov 1983] discussed general methods for determining the grasping forces and impulses in common gripper designs.

Impulsive forces and moments also cause instantaneous changes in the velocities of the linkages of the robot. These changes are functions of the impulses. If friction exists between the hand and the object, the generated impulses will depend on the modes of contact during impact. [Featherstone 1984] studied the motions of an open-loop system under impulsive forces. In his study, the effect of friction during impact is ignored. By applying the Coulomb friction law, [Chumenko and Yushchenko 1981] also derived general equations to describe the changes in velocities of generalized coordinates of a manipulator subject to impulses. They considered only two contact modes in impact: either the object sliding in the gripper, or sticking. The collision of the robot with its environment has

effects on the internal forces as well as on the velocities of the robotic system [Zheng and Hemami 1984].

With frictionless contact of objects and robot hands, the motion of an object is only influenced by the normal forces departed at the contact. With friction, on the other hand, the motion will be influenced in an involved way due to the tangential forces at the interface. The frictional forces can be very crucial to the motion of the object.

Mason investigated the effect of friction in robotic operations. By using the Coulomb model of friction, he found a technique to determine the motion of objects being pushed on a flat horizontal surface. The friction forces arise at the pushing contact and the supporting contact. During the pushing, the object will slide on the flat surface, and may or may not slip with respect to the pusher. Mason's method could determine which way the object will rotate without the knowledge of the supporting pressure distribution [Mason 1982; Mason 1986]. [Peshkin and Sanderson 1986] extended Mason's work by determining the locus of centers of rotation of the object for all possible distributions of support. The maximum pushing distance required to align an object can be found by using their approach.

Based on Mason's analysis, [Brost 1986] developed an automatic method for producing successful grasping plans. [Mani and Wilson 1985] also applied Mason's results and developed strategies for manipulation to orient parts being fed to a manufacturing process.

In Mason's analysis, inertial forces are assumed to be negligible. This constraint results in a simple mathematical model for the pushing operation. The analysis is valid when the speed of pushing or grasping is small enough, or the kinetic energy of the pushed object is rapidly dissipated [Mason 1985]. As the speed of motion increases, so do the inertial forces; as a result, the initial contact develops significant impulsive forces, and the process is no longer dominated by frictional forces alone. A dynamic model, rather than a quasi-static model, must be applied to analyze the operations involving fast speed and impact.

1.3. Overview

In section 2, we describe Coulomb's friction model and the coefficient of restitution that are used in this analysis. Other assumptions and the notations used in this paper are also described in this section. Section 3 discusses the impact process and Routh's technique which is used in the paper. Section 4 describes various modes of contact and the effects of the parameters of the process. Section 5 characterizes the motion of the object and the dynamic effects of the parameters on the motion. Finally, Section 6 concludes the analysis and offers some suggestions for further research.

2. Background and Notation

In order to explore the interaction of a robot and the objects in its surrounding world during impact, effective models of the interaction must be applied. In this section, we review a few physical concepts and make a few assumptions which will assure that the applied physical models are valid.

2.1. Friction

We will assume that the frictional interaction of objects is governed by Coulomb's law. The tangential force of friction generated during sliding is directed opposite to the direction of the motion, with magnitude proportional to the normal force. The constant of proportionality is called the coefficient of dynamic friction. If there is no sliding, the tangential force of friction is constrained to be no greater than the product of the normal force with the coefficient of static friction. Generally, static friction is slightly larger than dynamic friction. For impact processes, it is difficult to determine accurately the coefficients of dynamic friction. Consequently, the constants are specified either by pure hypothesis or by simplification. For the most simplicity, we use the coefficients for non-impact processes and the distinction between static and dynamic friction is ignored.

2.2. Coefficient of Restitution

A collision between two objects will produce a deformation. The deformation extends from the instant of contact to the maximum deformation. At the end of compression, the normal components of the relative velocity of the points of contact is zero. A period of restitution then will take place lasting to the termination of the impact. At the end of restitution, loss of contact occurs.

The magnitude of the normal impulse exerted at the contact point (P_n) consists of two parts, P_{nC} and P_{nR}, corresponding to the period of compression and the period of restitution, respectively. That is,

$$P_n = P_{nC} + P_{nR}. \tag{2.1}$$

The ratio of the magnitudes of P_{nR} and P_{nC} bears a constant e, which is given as

$$e = \frac{P_{nR}}{P_{nC}}. \tag{2.2}$$

The constant is called the coefficient of restitution. This relation is known as Poisson's hypothesis. If the vibrational effects of the impact are negligible, then the coefficient depends, to a large extent, only on the materials of the objects involved. The coefficient of restitution purports to describe the degree of plasticity of the collision, and its value is

always between 0 and 1. When $e = 0$, the impact is a perfectly plastic impact; when $e = 1$, the impact is a perfectly elastic impact.

If the centers of mass of the objects are located on the common normal of the surfaces in contact during the impact, then the coefficient of restitution can be evaluated by the initial and the final normal components of the relative velocity of the points of contact. The value of the coefficient is given as

$$e = -\frac{v_{cy}}{v_{cy_o}}, \tag{2.3}$$

where v_{cy_o} and v_{cy} are the initial and the final normal components of the relative velocity of the point of contact, respectively. This relation is called Newton's law.

Poisson's hypothesis and Newton's law give the same results for an eccentric impact if the object surfaces are perfectly smooth and frictionless (Beer and Johnston 1984). However, the two methods may not produce consistent solutions in general. In Appendix A, we show that the agreement holds if either of the following conditions is satisfied:

1. During the entire impact process, the contact keeps sliding and never reverses its direction.
2. The initial velocities of the points of contact are directed along the common normal to the surfaces in contact. That is, the impact is a directed impact.

Newton's method was used by [Whittaker 1904] to treat impacts with friction. [Kilmister and Reeve 1966] investigated both methods and stated that the extension of their agreement to smooth bodies is ultimate. However, the first condition presented here covers a broader class of impact than that of their statement. In other words, an impact of smooth bodies is a special case of the class of impact of the first condition. The second condition was also shown by [Keller 1986]. Both conditions represent the whole class of impact of the agreement of the two methods. Otherwise, they give inconsistent solutions. We define the coefficient of restitution by Poisson's hypothesis. The reason for this was pointed out by Kilmister and Reeve:

> *Experimentally there is not much to be said for either method of tackling the problem; but, from the point of view of logical structure in the laws of mechanics, Poisson's hypothesis is vastly preferable, since it states a dynamical law (it says that a certain impulse will act), whereas Newton's law states a constraint which it may be impossible to admit in a particular problem.*

2.3. Assumptions

A few assumptions are made to simplify the problem and to apply the above physical models:

- The object is constrained to planar motions.

- Frictional forces obey Coulomb's law.
- Local deformations at the contact point are not taken into account, and rolling friction is not considered.
- The number of collisions is restricted to one.
- The impact proceeds during a very short time interval and the process is dominated by the impulsive forces produced during the impact. The object has no displacement during the interval.
- The transformation of the initial kinetic energy of the system into vibrations of the striking bodies is negligible. This is reasonably valid for collisions of large bodies, but not for the collisions involving a rod, beam or thin plate [Goldsmith 1959].

The approach of this paper is based primarily on the impulse-momentum law for rigid bodies. It specifies the final velocity state of the object after impact and determines the impulses applied to the object. This approach is incapable of describing the transient impulsive forces and the deformations produced during the impact.

2.4. Notation

In Figure 3.1, we illustrate the notation that will be used to describe the processes of impact:

θ	angle of object measured with respect to the common normal of contact.
γ	angle of the incident velocity of the point of contact measured with respect to the common normal.
γ_r	angle of the rebound velocity of the point of contact measured with respect to the common normal.
$\mathbf{v}$	velocity of center of mass.
$\mathbf{v}_o$	initial velocity of center of mass.
$\mathbf{v}_c$	velocity of the point of contact.
$\mathbf{v}_{co}$	initial velocity of the point of contact.
ω	angular velocity of object.
ω_o	initial angular velocity of object.
m	mass of object.
ρ	radius of gyration.
l	distance from the center of mass to the contact point.
μ	coefficient of friction.
α	friction angle. $\tan\alpha = \mu$.
e	coefficient of restitution.
P_t	tangential component of impulse.
P_n	normal component of impulse.

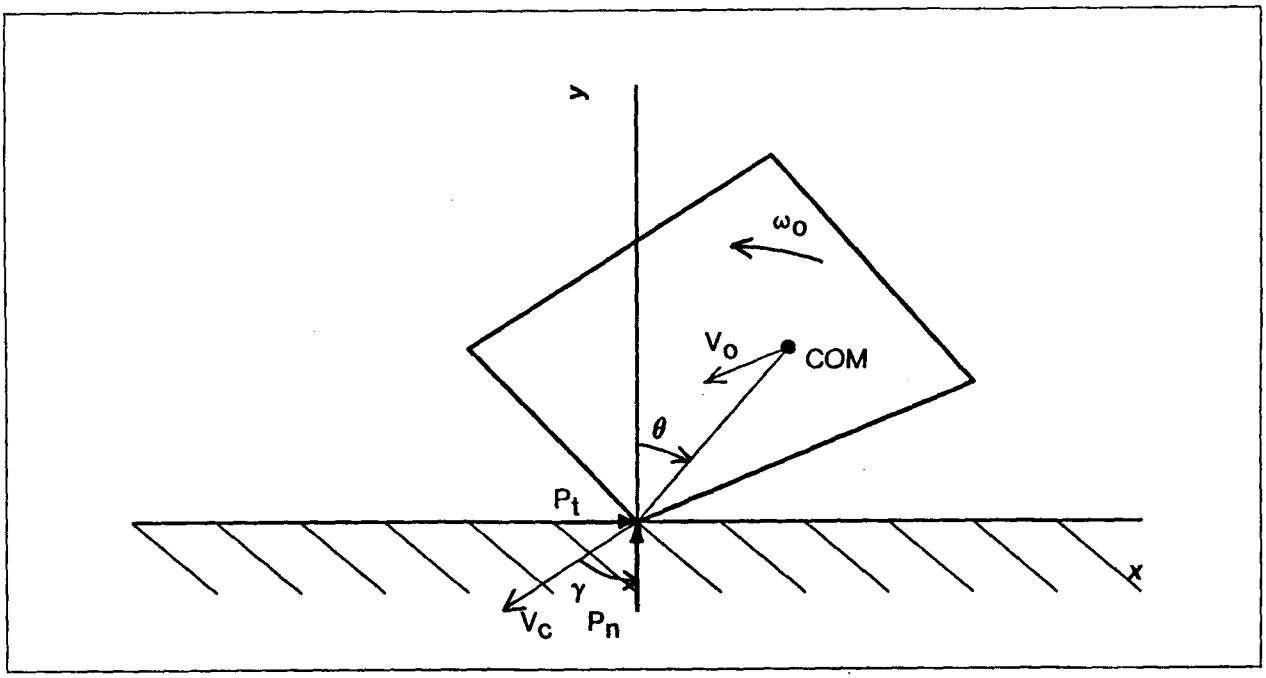


Figure 3.1. A polygonal object strikes a flat constraint surface. With the initial geometrical terms $\mathbf{v}_o$ and ω_o, the object is subject to the normal and the tangential impulses P_n and P_t during the process of impact.

3. Analysis of Impact Process

This section analyzes the impact process of a rigid object striking another fixed object. In the general case there is only one point of contact between two colliding objects. The normal component of the resulting impulsive force lies in the common normal of the surfaces at the point. We assume that the fixed object has a flat surface. Contact occurs between a corner of the moving object and the surface of the fixed object (Figure 3.1). Without loss of generality, the analysis applies when a surface of the moving object is in contact with a point of the fixed object, and when the second object is also in motion. In this section we first restate Routh's method and then present all possible cases of impact cases. An example is used to illustrate the technique.

3.1. Dynamic Equations of Motion

When the object strikes the surface, impulses in the normal direction and in the tangential direction at the contact point are produced. These impulses will change the motion of the object. As shown in Figure 3.1, the initial translational and rotational velocity components of the object are v_{xo}, v_{yo}, and ω_o. The origin of the coordinates is chosen at the point of contact. The coordinate axes are in the directions tangential and normal to the contact surfaces. Positive values of P_t are chosen to the right. At any time during the impact the motion of the object is governed by the linear and angular

impulse-momentum laws, which provide the following relations:

$$\left.\begin{aligned} m(v_x - v_{xo}) &= P_t \\ m(v_y - v_{yo}) &= P_n \\ m\rho^2(\omega - \omega_o) &= P_t y - P_n x \end{aligned}\right\} \tag{3.1}$$

where ρ is the radius of gyration of the object, and x, y are the coordinates of the center of mass (COM).

The velocity of the point in contact consists of two components, the sliding velocity v_{cx} in the tangential direction and the compression velocity v_{cy} in normal direction. These two components are given by

$$v_{cx} = v_x + y\omega \tag{3.2}$$

$$v_{cy} = v_y - x\omega \tag{3.3}$$

Substituting the dynamic equations (3.1) into these equations, we fine that

$$v_{cx} = v_{cxo} + B_1 P_t - B_3 P_n \tag{3.4}$$

$$v_{cy} = v_{cy_o} - B_3 P_t + B_2 P_n \tag{3.5}$$

where

$$v_{cxo} = v_{xo} + y\omega_o \tag{3.6}$$

$$v_{cy_o} = v_{yo} - x\omega_o \tag{3.7}$$

$$\left.\begin{aligned} B_1 &= \frac{1}{m} + \frac{y^2}{m\rho^2} = \frac{\rho^2 + y^2}{m\rho^2} \\ B_2 &= \frac{1}{m} + \frac{x^2}{m\rho^2} = \frac{\rho^2 + x^2}{m\rho^2} \\ B_3 &= \frac{xy}{m\rho^2} \end{aligned}\right\} \tag{3.8}$$

These are the initial descriptions for the impact process, and v_{cxo} and v_{cy_o} represent the initial velocities of sliding and compression. The value of v_{cy_o} must be negative so that the object is striking the surface. B_1, B_2, and B_3 are constants independent of the initial motion of the object. They are dependent on the position of the center of mass. It is evident that B_1 and B_2 are positive. B_3 may be either positive or negative depending on where the center of mass is.

3.2. Force Constraints

In the dynamic equations of motion (3.1), there are five unknowns: three velocities and two impulses. To solve the equations two additional constraints are required. The

constraints may be geometrical ones or force ones. At the left side of equation (3.1) are the changes in the translational and rotational velocities of the object during impact. These changes are determined by the amplitudes of the normal and the tangential impulses at the right side of equation (3.1). These impulses are governed by the properties of the object and the surface. In general, the striking surfaces are partially elastic and imperfectly smooth.

3.2.1. Elasticity Constraint

The first constraint is the elastic property of the object. As we have discussed in Section 2.2, the coefficient of restitution leads to a force constraint to the final normal impulse P_n. Substituting equation (2.2) into equation (2.1), we obtain

$$P_n = (1+e)P_{nC} \tag{3.9}$$

where P_{nC} is the magnitude of the accumulated normal impulse at the instant of maximum compression. At that instant, the normal velocity of the point in contact is zero and the period of compression is terminated. Letting $v_{cy} = 0$ in equation (3.5), we obtain

$$v_{cy_o} + B_3 P_{tC} - B_2 P_{nC} = 0 \tag{3.10}$$

This equation shows that the normal and the tangential impulses are in a linear relationship at the instant of maximum compression.

If either of the conditions for the agreement of Poisson's and Newton's methods is satisfied (see Section 2.2), then the force constraint can be expressed by a geometric constraint. The final normal component of the velocity at the point of contact can be obtained directly from equation (2.3), which yields

$$v_{cy} = -e v_{cy_o} \tag{3.11}$$

Substituting this into equation (3.5), we obtain a linear equation representing the conditions for the termination of the process of the impact as

$$(1+e)v_{cy_o} + B_3 P_t - B_2 P_n = 0 \tag{3.12}$$

Note this equation is only valid when either of the above mentioned conditions holds. If so, then it is equivalent to the constraint given by equation (3.9) to determine the termination of the process.

3.2.2. Friction Constraint

The second constraint is the friction of the surfaces. When the surfaces are not perfectly smooth, a frictional impulse will be called into play in the impact process. As a consequence of Coulomb's law, sliding of the points in contact occurs when $|F_t| = \mu F_n$,

while sticking occurs when $|F_t| < \mu F_n$. Here F_t and F_n are the impulsive forces in the normal and the tangential directions. In the latter case, the object is rolling across the surface, and the tangential velocity of the point of contact is zero. Letting $v_{cx} = 0$ in equation (3.4), we obtain the relation of the impulses for the sticking contact as follows:

$$v_{cxo} - B_1 P_t + B_3 P_n = 0 \tag{3.13}$$

The relation of the impulses is also linear.

If the object slides over the surface at the beginning of the impact, the impulses will increase from their zero initial values with the following relation

$$|P_t| = \mu P_n \tag{3.14}$$

P_n increases monotonicly in time. Coulomb's law says that the increment (dP_n, dP_t) obeys the relation:

$$|dP_t| = \mu dP_n \tag{3.15}$$

If the surface is rough enough, this relation cannot hold throughout the whole process of the impact. The increment dP_t may be just sufficient to prevent further sliding of the point of contact. In this case, enough friction is generated to keep the point in contact at rest. The object therefore will roll across the surface. The impulsive frictional force is no longer in its limiting value, and a discontinuity of the force may arise. The relationship between the increments of the impulses is give by

$$|dP_t| < \mu dP_n \tag{3.16}$$

As long as this relation is satisfied, the object will roll and will continue to roll across the surface and the impulses P_t and P_n will be constrained by equation (3.13).

3.3. Impact process Diagram

To determine the actual changes which occur in the frictional impulse as the impact proceeds, we apply a graphical technique developed by [Routh 1860], as shown by an example in Figure 3.2. In the impact process diagram, a rectangular coordinate system with P_t as the horizontal axis and P_n as the vertical axis represents an impulse space, and a representive point P describes the accumulated impulse of the object at any moment of the impact. The set of all possible impulse states forms the well-defined *impulse space.* Starting with the origin O, which indicates the zero initial impulse, the representive point P will travel along a path with the normal impulse P_n increasing. The positive motion of P along the horizontal axis correspond to an object sliding to the left in Figure 3.1.

Equations (3.10), (3.12), and (3.13) describe straight lines in the diagram. We call these line of maximum compression, line of termination, and line of sticking, respectively,

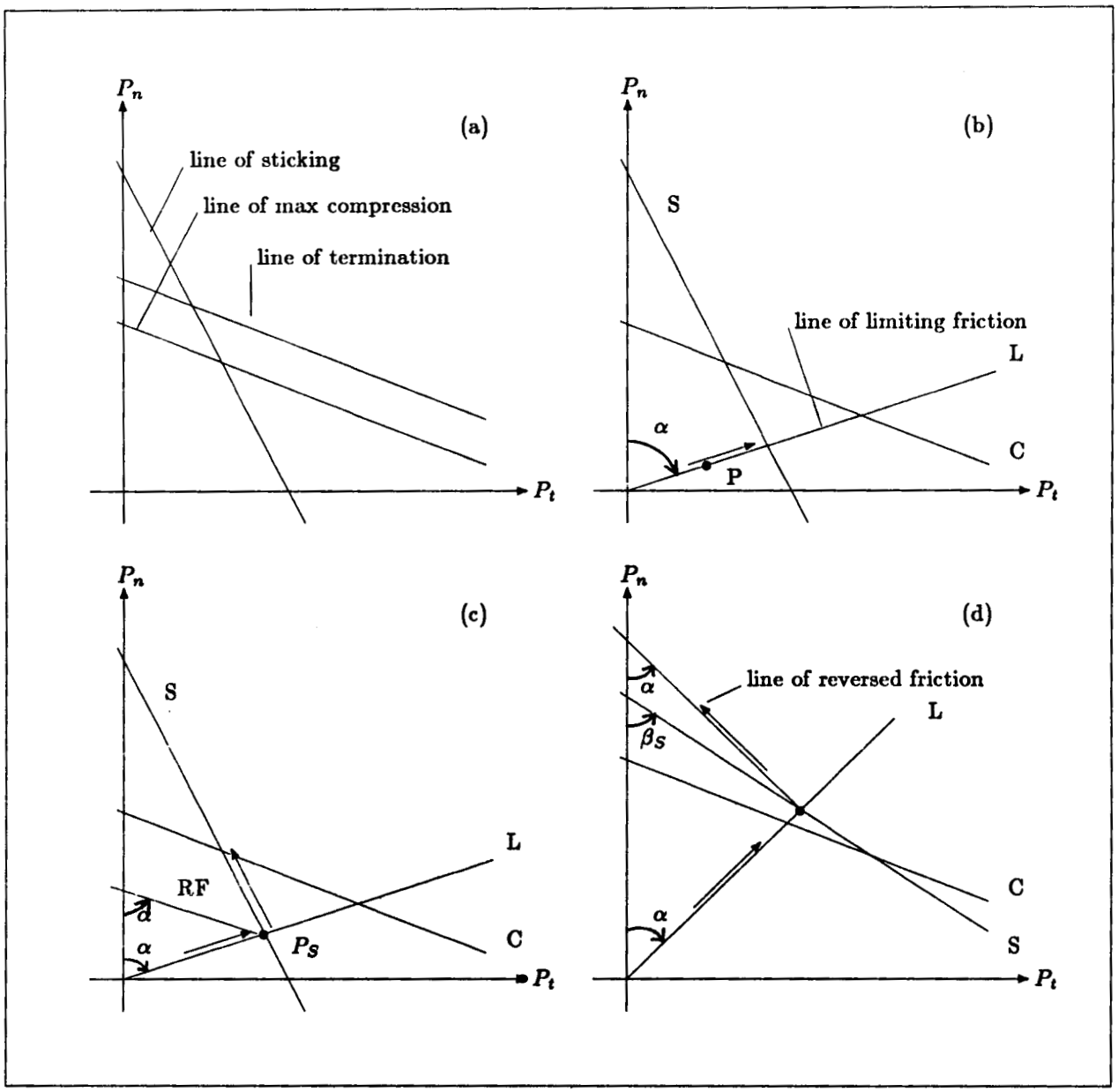


Figure 3.2. Impact process diagrams. The representive point travels along the limiting friction line (b). If the limiting friction is enough to prevent sliding, then it follows the line of sticking after intersecting with it (c). If it is not enough, then the point changes to the line of reversed friction (d). The lines of sticking, lines of maximum compression, and lines of termination are labeled respectively with S, C, and T. The lines of limiting friction and the lines of reversed limiting friction are labeled with L and RF respectively.

as shown in Figure 3.2a. Note the line of termination is only good for the impact in which either conditions for the agreement of Poisson's method and Newton's method is met. Now we can trace the path of P. At the beginning of the impact the object is sliding over the surface, hence the maximum frictional impulse $P_t = \mu P_n$ is developed. Therefore, the representive point P will travel in the direction of increasing P_n along the line of

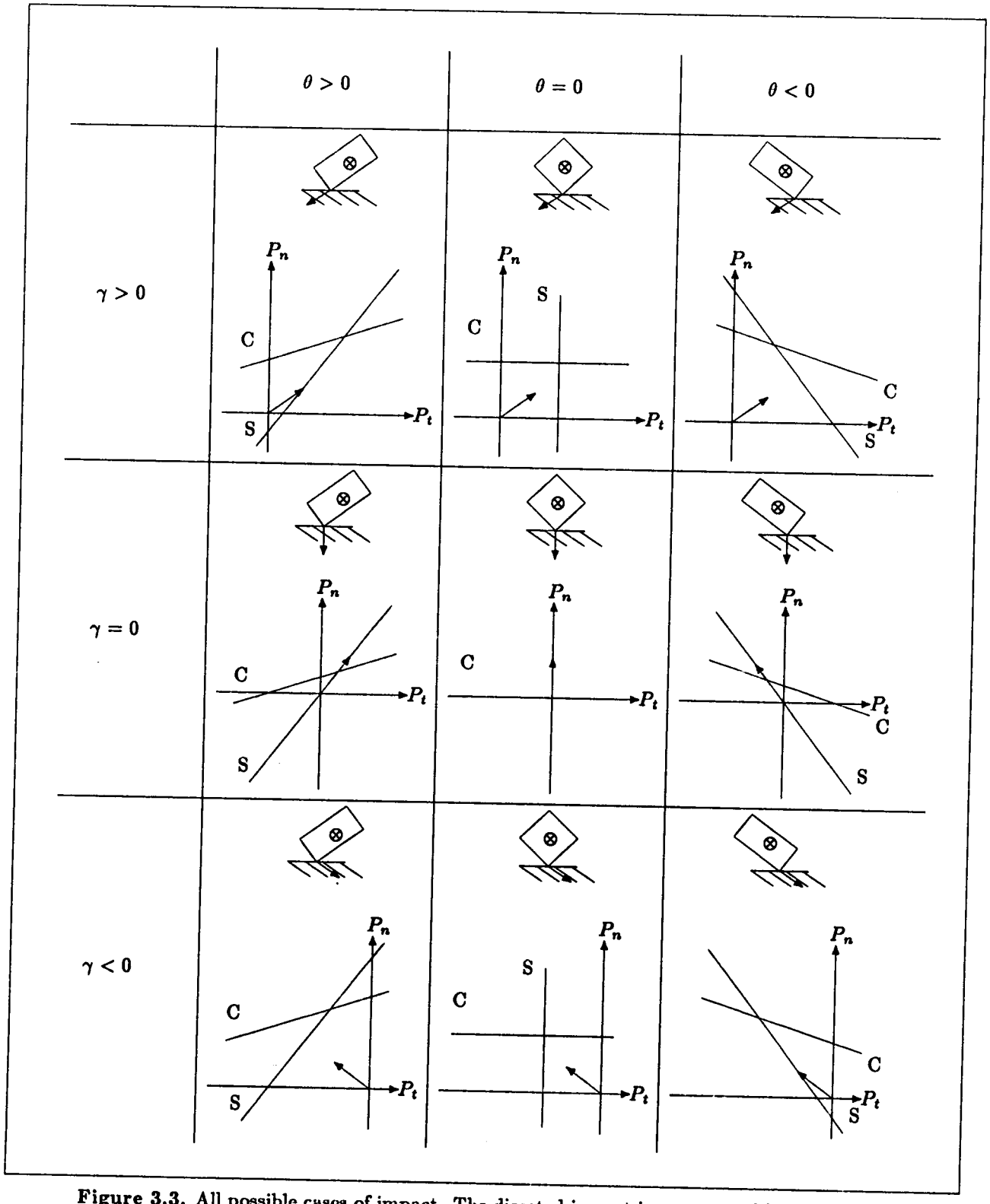


Figure 3.3. All possible cases of impact. The directed impact is represented by the second row where $\gamma = 0$, while the central impact is represented by the second column where $\theta = 0$. Others represent general impact processes. The lines with label S are lines of sticking, Those with label C are lines of maximum compression.

limiting friction which is defined by equation (3.14) (Figure 3.2b). The friction continues to be limiting until P reaches the line of sticking. At the intersection point P_S, the initial sliding phase is ended. Beyond P_S, the friction will exhibit a change as discussed in Section 3.2.2.

The principle that determines the path of the point is that only as much friction will act as is necessary to prevent sliding, provided this is less than the value of the limiting friction. There are two possible cases. In Figure 3.2c, the friction necessary to prevent sliding is less than the limiting friction. Hence, P will follow the line of sticking until the termination of the process. In this case, the maximum friction is not required. In Figure 3.2d, however, the friction necessary to prevent sliding is larger than the maximum available. The friction therefore will change its direction and maintain its limiting value. Point P, after reaching P_S, will travel along the line of reversed limiting friction.

Then, point P will continue to follow the line as before, but we note the value of P_{nC} as it crosses the line of maximum compression, and terminates when P_n is $(1+e)$ times that value. This is the elasticity constraint given by equation (3.9).

In Figure 3.3 we illustrate nine possible cases of impact processes. The rows are represented in terms of direction of relative velocity of point at contact, while the columns are represented in terms of the relative location of the center of mass. Likewise, the middle row (where $\gamma = 0$) represents the directed impact, while the middle column (where $\theta = 0$) represents the central impact. Others are the eccentric oblique impacts.

3.4. An Example

To illustrate how to use the impact process diagram to solve impact problems, we show an example. Consider a sphere of mass m moving down to the left with a velocity $\mathbf{v}_o$ at an angle γ with the vertical axis y (Figure 3.5). This is the case of central oblique impact ($\gamma > 0$ and $\theta = 0$ in Figure 3.3). When the sphere strikes the surface, it can bounce up as well as slide to the left. We can use the impact process diagram to determine the motion of the sphere.

Two possible cases are separated by the angle ϕ, which is given by

$$\tan\phi = \frac{1}{(1+e)}\tan\gamma \tag{3.17}$$

If the friction angle $\alpha > \phi$, the representive point P will first travel along the line of limiting friction to the intersection with the line of sticking. The sphere stops sliding and rolls on the surface. P will then continue to move along the line of sticking beyond the end of compression and to the termination of the process. Figure 3.4a shows the procedure. We can rewrite the condition of this case as

$$\tan\gamma < (1+e)\tan\alpha \tag{3.18}$$

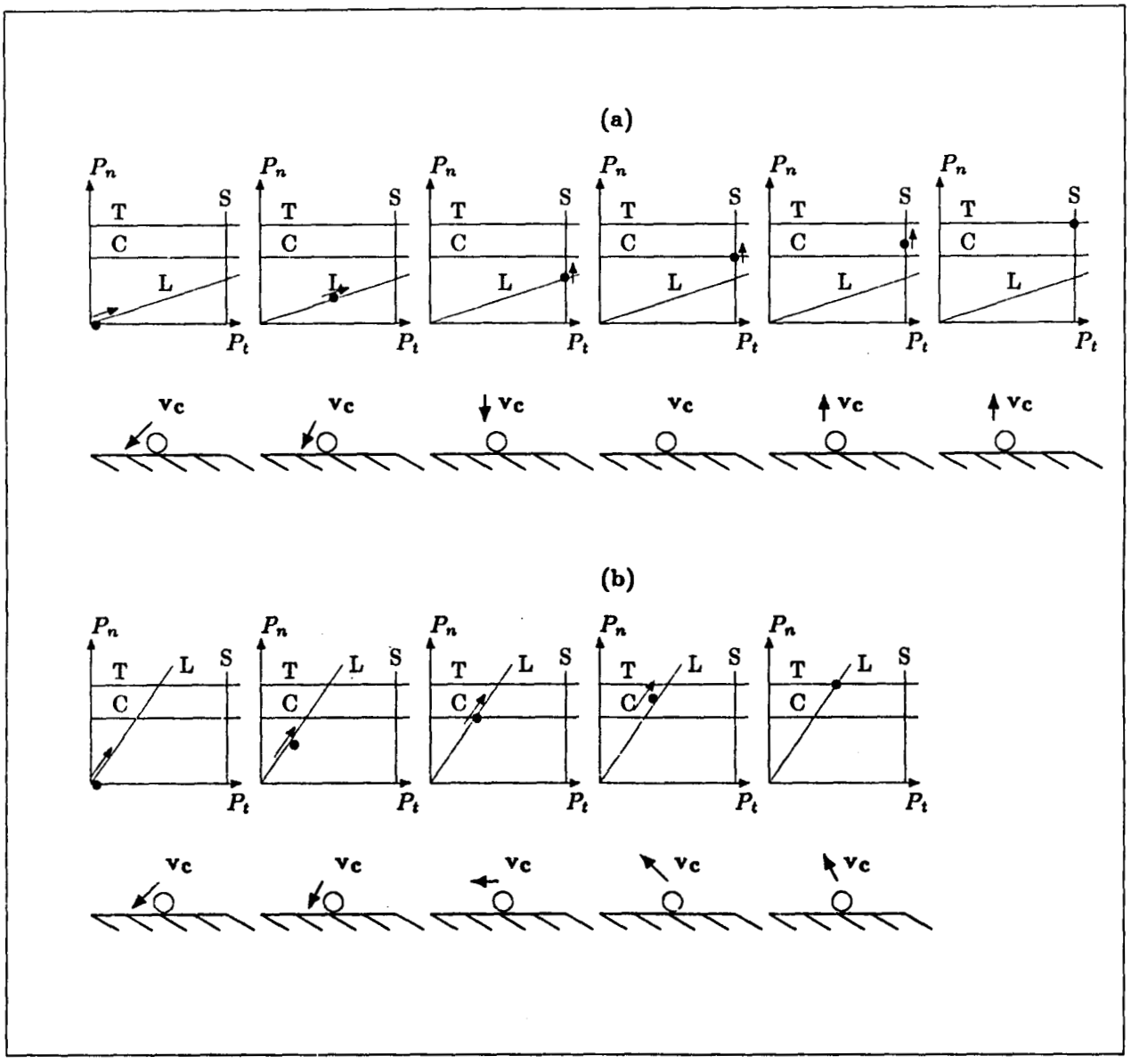


Figure 3.4. The example of a sphere striking a constraint surface. In case (a), the relative tangential velocity of the point of contact is stopped in the process, and the sphere rolls on the surface. In case (b), the sphere keeps sliding during whole period of the process, and is reflected to the left. Again, we label lines of sticking with S, lines of maximum compression with C, and lines of termination with T. The lines of limiting friction are labeled with L.

or

$$\gamma < \alpha_e \tag{3.19}$$

where angle α_e is called the *effective friction angle*, defined as

$$\tan \alpha_e = (1 + e) \tan \alpha \tag{3.20}$$

The effective friction angle takes into account both surface properties: elasticity and roughness. If the surface is perfectly plastic, i.e., $e = 0$, then α_e is the real friction angle.

Otherwise, the value of the effective friction angle is greater than that of the real friction angle.

In this case, in which the initial velocity angle γ is less than the angle α_e, we see that the velocity of the point of contact $\mathbf{v}_c$ will be straight up in the normal direction, and that the final impulse will lie in the interior of the real friction cone as shown in Figure 3.5a. The motion of the sphear after impact is independent of the coefficient of friction μ, since sufficient friction to prevent sliding is called into play in the process. Further increases in μ have no physical effect.

If $\alpha < \phi$, point P will travel along line of limiting friction in Figure 3.4b and the process will be terminated before it reaches the line of sticking. The sphere slides to the left, as well as bounces up. The direction of the motion of the point of contact makes an angle γ_r with the normal direction. The relation between the angles γ_r and γ is defined by

$$\tan\gamma - e\tan\gamma_r = \mu(1+e) \tag{3.21}$$

or

$$\tan\gamma - e\tan\gamma_r = \tan\alpha_e \tag{3.22}$$

In this case, $\gamma > \alpha_e$. The final impulse lies on the edge of the real friction cone as shown in Figure 3.5b.

3.5. Summary

In the previous example, several variations of the impact process have been shown. A great variety of cases can occur depending on the geometric configuration of the process and the friction coefficient μ. The path of the representive point P may change from one of the lines (line of sticking, of maximum compression, and of limiting friction) to another, depending on where the lines intersect. The progress of an impact can be traced by the method, which may be summed up in the following rules:

1. The representive point P will always travel in the direction of increasing the normal component of the impulse.
2. Initially, it proceeds from the origin along the line of maximum friction if it is not a directed impact. Otherwise, along the line of sticking.
3. Compression is terminated when the representive point reaches the line of maximum compression, and then restitution starts.
4. The process is terminated when the normal impulse reaches the final value $P_n = (1+e)P_{nC}$.
5. If the representive point meets the line of sticking, the point continues along either the line of sticking or the line of reversed limiting friction, whichever is steeper to the

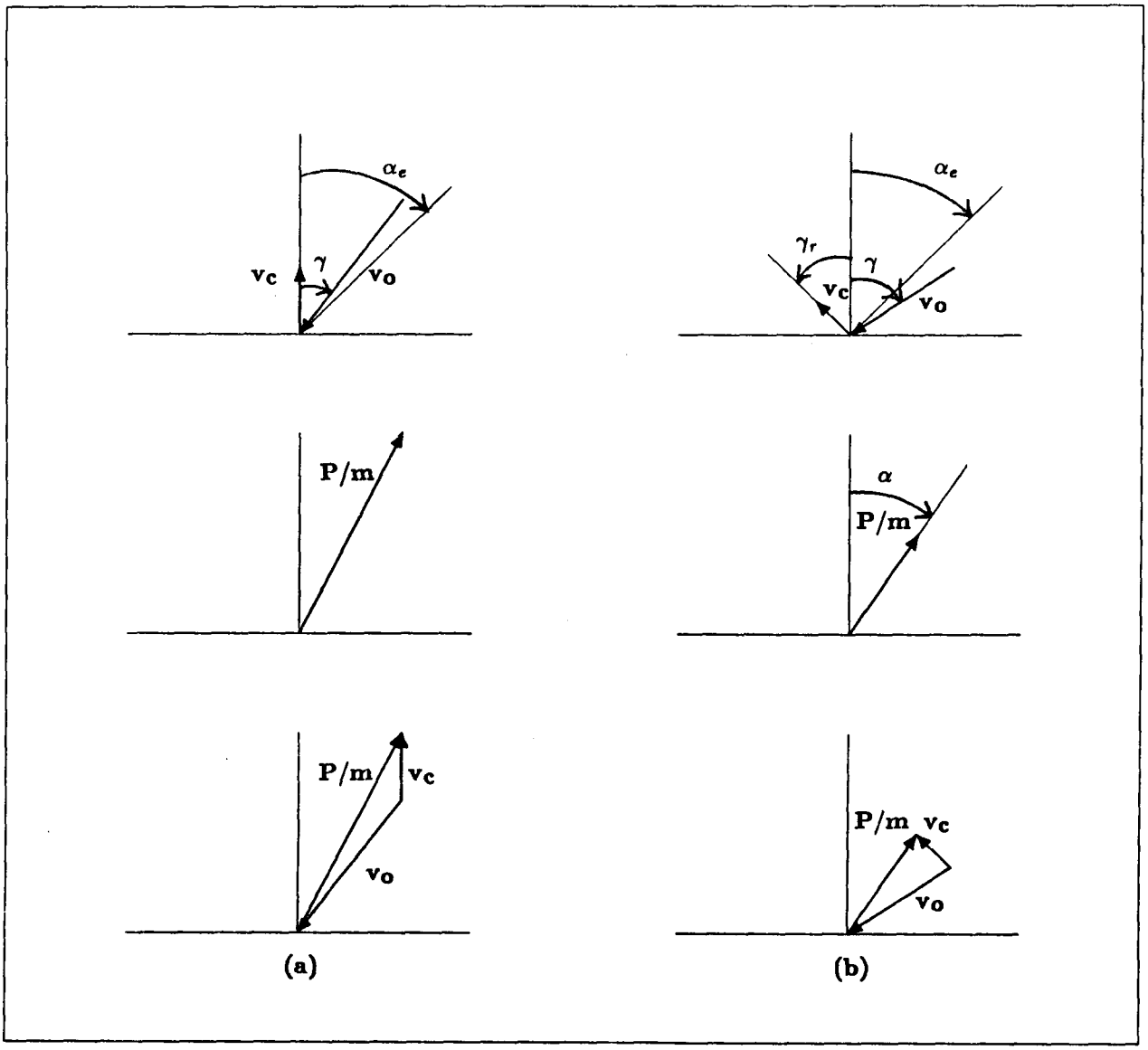


Figure 3.5. Motions of the sphere and the impulse. In case (a), the initial velocity lies in the effective friction cone, the sphere will roll on the surface. In case (b), the initial velocity lies outside of the effective friction cone, the sphere will slide to the left as well as bounce up.

axis of P_n.

6. The friction reverses its direction when point P starts to travel along the line of reversed limiting friction.

7. The friction may reverse its direction, but only once.

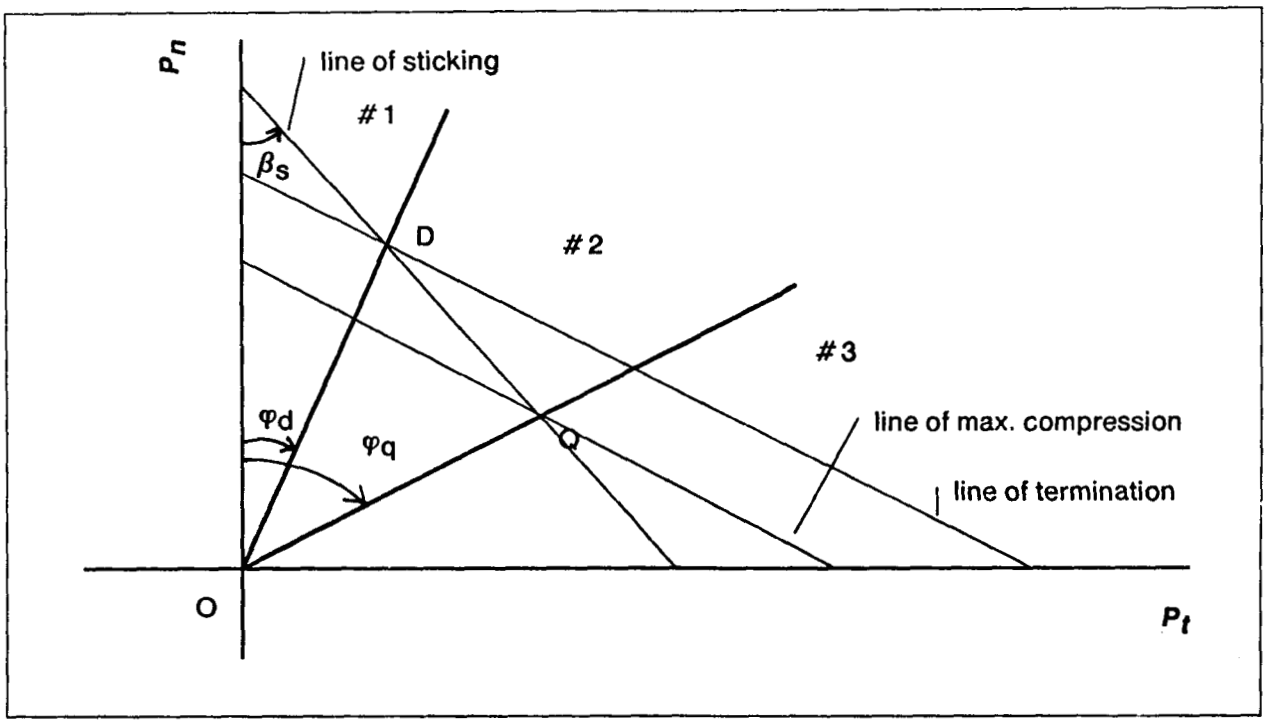


Figure 4.1. The three major regions of impact. In region 1, sticking never occurs; in region 2 and region 3, the impact process is terminated with no relative tangential motions at the point of contact.

4. Contact Modes of Impact

In the previous sections, we saw that a variety of contact modes may occur for an impact process. The actual mode of contact depends on the striking velocity, the position of the center of mass of the object, the coefficient of friction μ, and the coefficient of restitution e. Given these parameters we can predict the net impulse generated in an impact. However, impulse space only allows descriptions of the process in a produced impulse domain. For a variety of geometric configurations it is not easy to predict the contact conditions in the space. The effects of the parameters on the contact conditions are also not well illustrated. In this section, we present an impact space constructed by the geometric description of the impact: the direction of the striking velocity and the angular position of the the center of mass of the object. In this space, the contact mode and the motion of the object for all possible striking moves can be predicted, and the effects of the parameters on them are well shown.

4.1. Impact Space

We start with an analysis of a general impact process. In Figure 4.1 the general process is represented by the impact process diagram. The impulse space is divided into three regions by the lines OD and OQ. If the limiting friction line lies in region 1, the impact will be terminated before the representive point P reaches the line of sticking. The

friction continues the limiting value throughout the process, so that the object slides on the constraint surface throughout. If the point starts traveling along a line of limiting friction which lies in region 2, it reaches the line of maximum compression first, then reaches the line of sticking. If the line of limiting friction lies in region 3, it reaches the line of sticking first. In either regions, 2 or 3, after intersecting with the sticking line, it either continues sticking until termination or undergoes reversal sliding.

Table 4.1 Categories of Contact Modes		
	$\alpha < \beta_S$	$\alpha > \beta_s$
$\alpha < \phi_d$	Sliding	Sliding
$\phi_d < \alpha < \phi_q$	R-sticking	R-reversed Sliding
$\alpha > \phi_q$	C-sticking	C-reversed Sliding

Table 4.1 illustrates major categories of the contact modes. The difference between R-sticking and C-sticking is made upon the period during which the tangential relative motion of the contact point is stopped. If it is stopped during the period of restitution, then the contact is called the restitution sticking (R-sticking) contact; if it is stopped during the period of compression, then the contact is called the compression (C-sticking) contact. In a similar way, R-reversed sliding and C-reversed sliding contacts differ. Later in Section 5.1, we will see that the object has different motion cheracteristics for these distinct contact modes.

The necessary and sufficient condition for sliding contact (in region 1) can be rewritten in terms of the geometric descriptions of the process as follows

$$\begin{aligned}(1+r^2)\tan\gamma\,\tan^2\theta - r^2\mu\tan\gamma\tan\theta + \tan\gamma \\ -\mu(1+e)\tan^2\theta + r^2(1+e)\tan\theta > \mu(1+e)(1+r^2) \\ \text{for } \gamma \geq 0\end{aligned} \tag{4.1}$$

where r is the ratio given by $r = l/\rho$. Similarly, the condition for the reversed sliding contacts is that

$$\mu\tan^2\theta - r^2\tan\theta + \mu(1+r^2) < 0 \tag{4.2}$$

Again, for C-sticking contact, the conditions can be expressed as follows

$$\begin{aligned}(1+r^2)\tan\gamma\tan^2\theta - r^2\mu\tan\gamma\tan\theta + \tan\gamma \\ -\mu\tan^2\theta + r^2\tan\theta < \mu(1+r^2).\end{aligned} \tag{4.3}$$

In the relations given by (4.1), (4.2), and (4.3), the angle θ is the orientation of the object, measured relative to the normal of the surface (see Figure 3.1). The angle γ defines

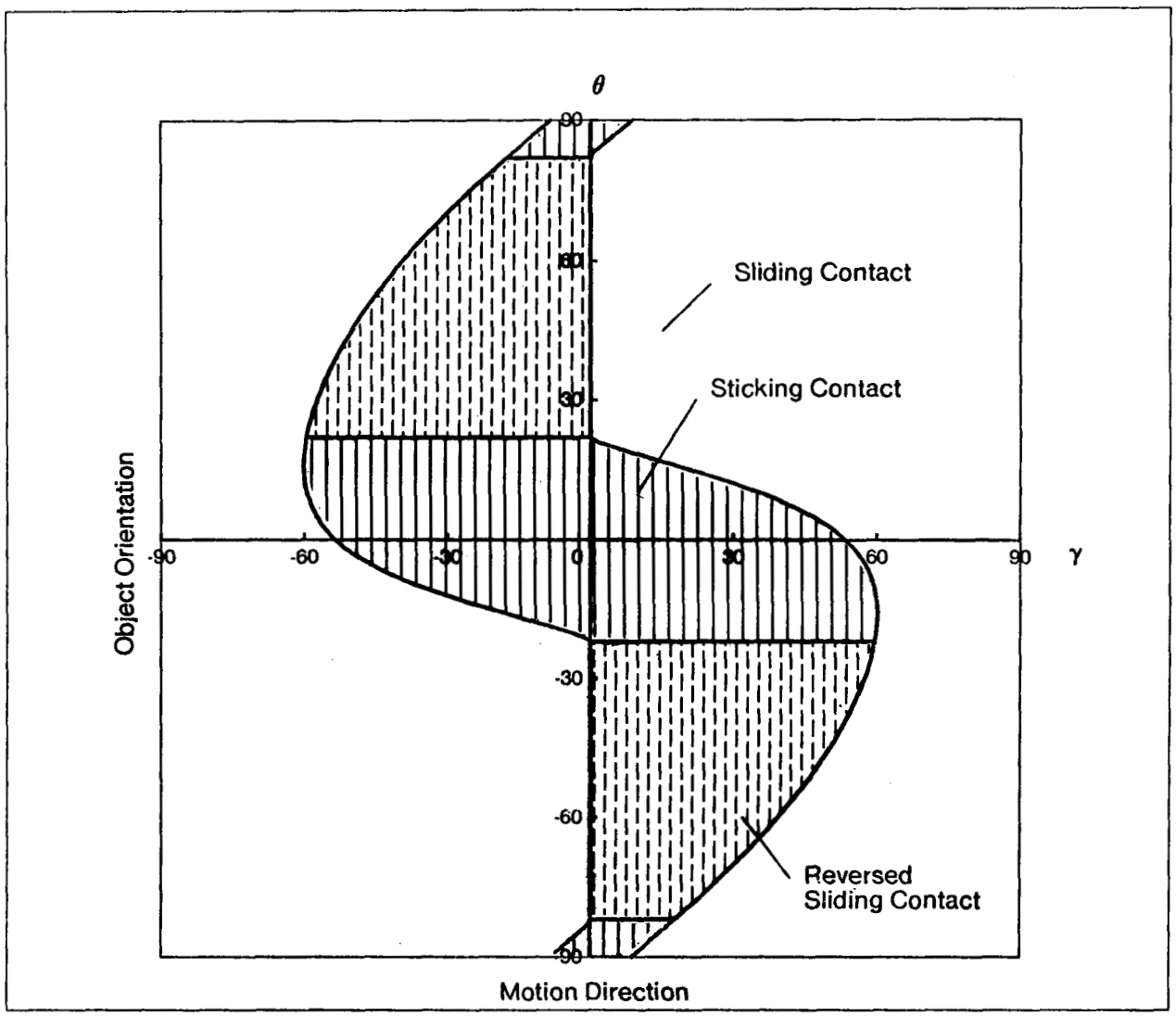


Figure 4.2. Impact space. The γ - θ coordinate system represents all possible impact states. The impact space is divided by the regions of contact modes. In this example, $\mu = 0.25, e = 0.8$, and $r = 1.414$.

the direction of striking of the object. θ ranges from -90 to 90 degrees, while γ ranges from 0 to 90 degrees. For convenience, we define that γ is positive when the object strikes the constraint surface from the right to the left. If the striking is from the left to the right, i.e., $\gamma < 0$, the solutions are identical to those of positive γ, but of negative θ. Thus, the range of γ can be extended, by the symmetry, to that from -90 to 90 degrees.

Note that a set of γ and θ represents a state of striking. The set of all possible striking moves forms a well-defined *impact space*. A rectangular coordinate system with γ as the horizontal axis and θ as the vertical axis can represent the impact space. Relations (4.1), (4.2), and (4.3) represent the regions of sliding contact, sticking contact, and reversed sliding contact (Figure 4.2). We can fully determine the contact mode of an impact from

the geometric configurations of the operation in the impact space.

An example of impact space is shown in Figure 4.2. The space consists of the regions of these three contact modes as labeled. The ambiguous cases occur when the striking state is on the boundaries between these regions.

4.2. Effects of the Parameters

Three dimensionless parameters are defined to describe the properties of the object. The parameters, μ, e, and r determine the possible modes of contact and the boundaries between the contact regions. Consequently, the motion of the object after impact is affected by the values of the parameters.

One of these parameters, $r = l/\rho$, is a dimentionless quantity that represents the effectiveness of the moment of inertia referred to the point of contact. For a larger value of r, the motion of the point of contact has large changes with the change of the orientation of the center of mass. It makes sliding or reversed sliding more likely to occur. Figure 4.3a shows an example for large value of r. Most regions in the impact space are for sliding contact or reversed sliding contact.

Smaller value of r makes sticking contact more likely to occur. On the other hand, the smaller the value of r, the less possible that the contact will reverse its direction. More exactly, reversed sliding contact occurs only when

$$\frac{r^2}{\sqrt{1+r^2}} > 2\mu \tag{4.4}$$

When reversed sliding does not occurs, sticking will occur for all orientations from -90 to 90 degrees as shown in Figure 4.3b. If the contact point lies on the center of mass, i.e., $r = 0$, the contact modes and motion of the object are then independent of the the orientation of the object (Figure 4.3c).

Other parameters are the coefficient of restitution e and the coefficient of friction μ. For a perfect plastic impact, i.e., $e = 0$, the restitution period of the process does not exist. Correspondingly, the R-sticking contact and the R-reversed sliding contact do not exist. Elasticity of the object provides an opportunity for the initial sliding to be stopped during the period of restitution. Hence, a large value of e enlarges the regions of sticking and reversed sliding contact as illustrated in Figure 4.4.

Basically, friction resists the sliding of the object. If the surface is very rough (high μ), most states of impact stick, while only very large angle of incidence (γ) may produce sliding at the contact point. Figure 4.5 shows an example of large friction, where sliding contact occurs at very large angles of incidence.

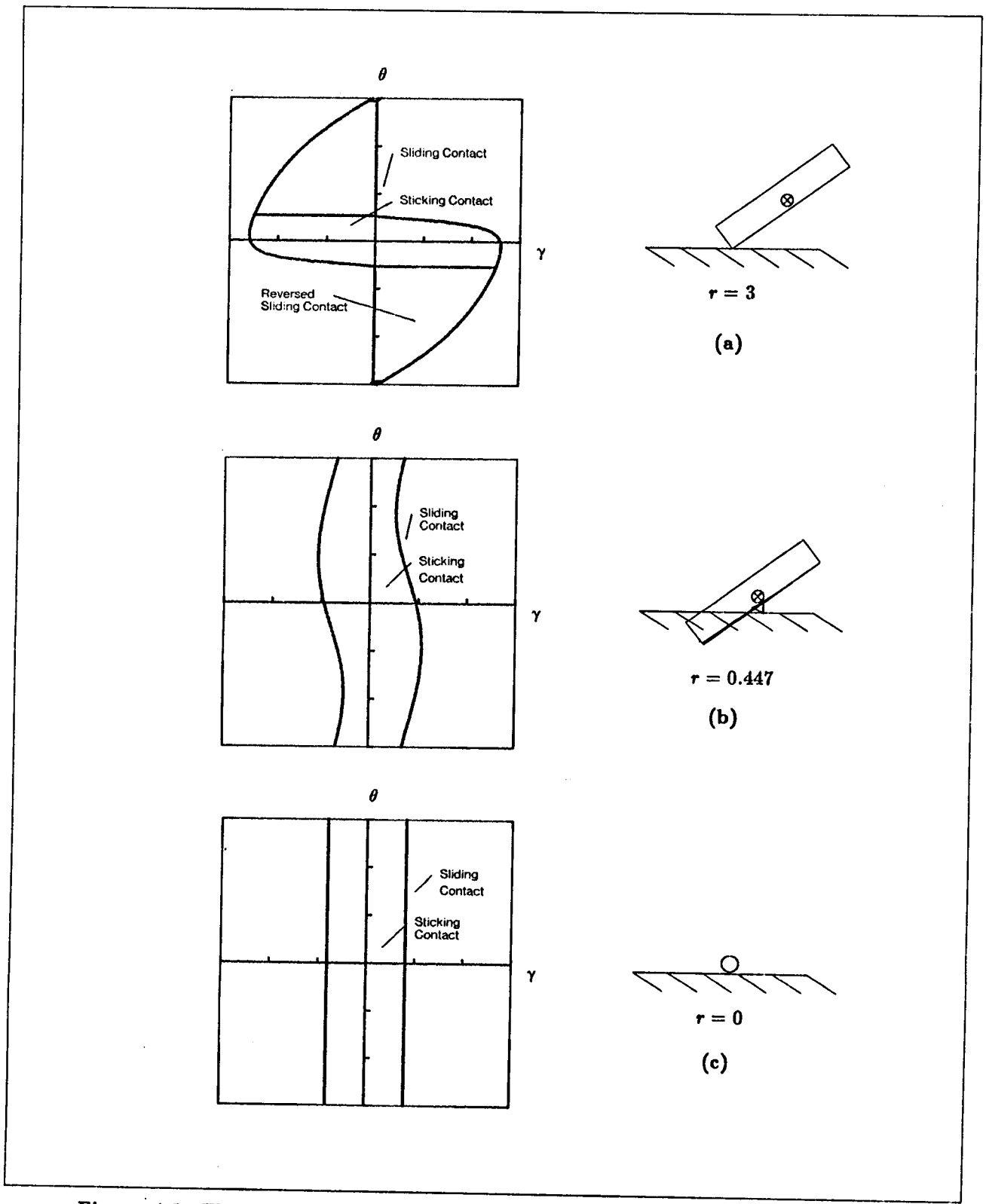


Figure 4.3. The effect of the value of r. Here $r = 3$ for case (a), $r = 0.447$ for case (b), and $r = 0$ for case (c). In all cases, $\mu = 0.25$, and $e = 0.8$.

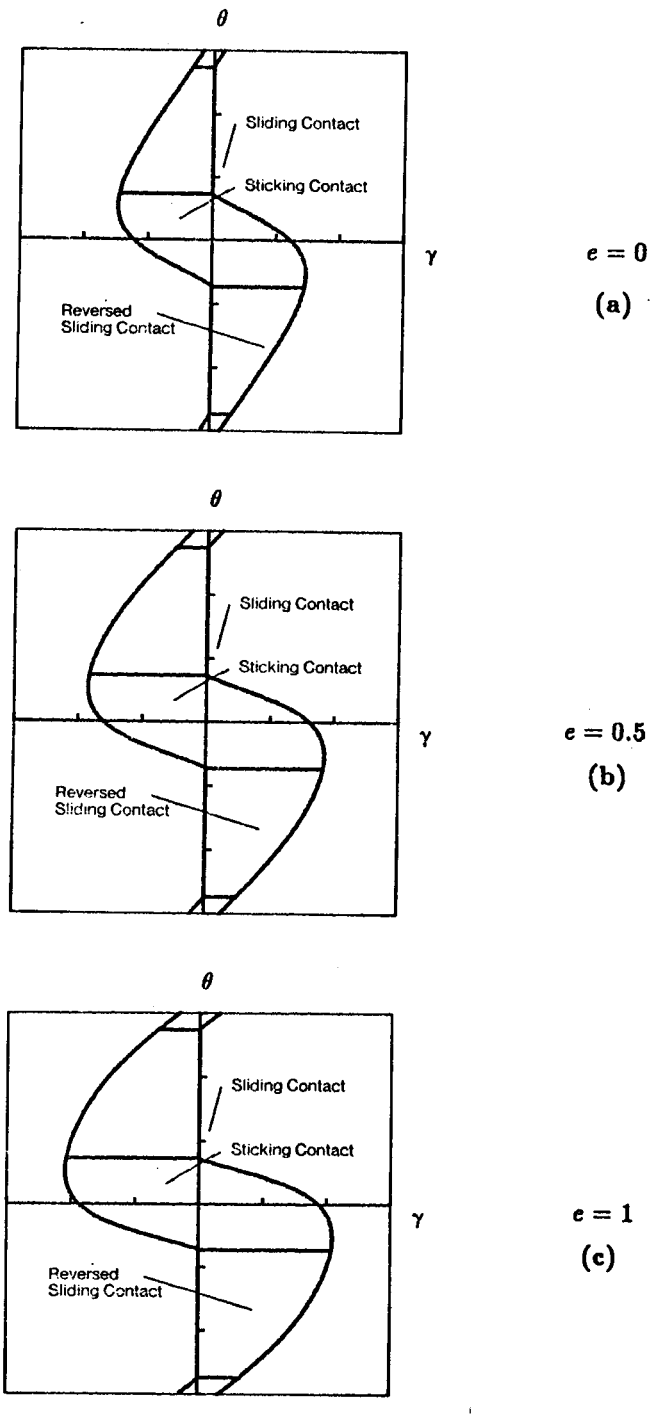


Figure 4.4. The effect of the coefficient of restitution. Here $e = 0$ for case (a), $e = 0.5$ for case (b), and $e = 1$ for case (c). In all cases, $\mu = 0.25$, and $r = 1.414$.

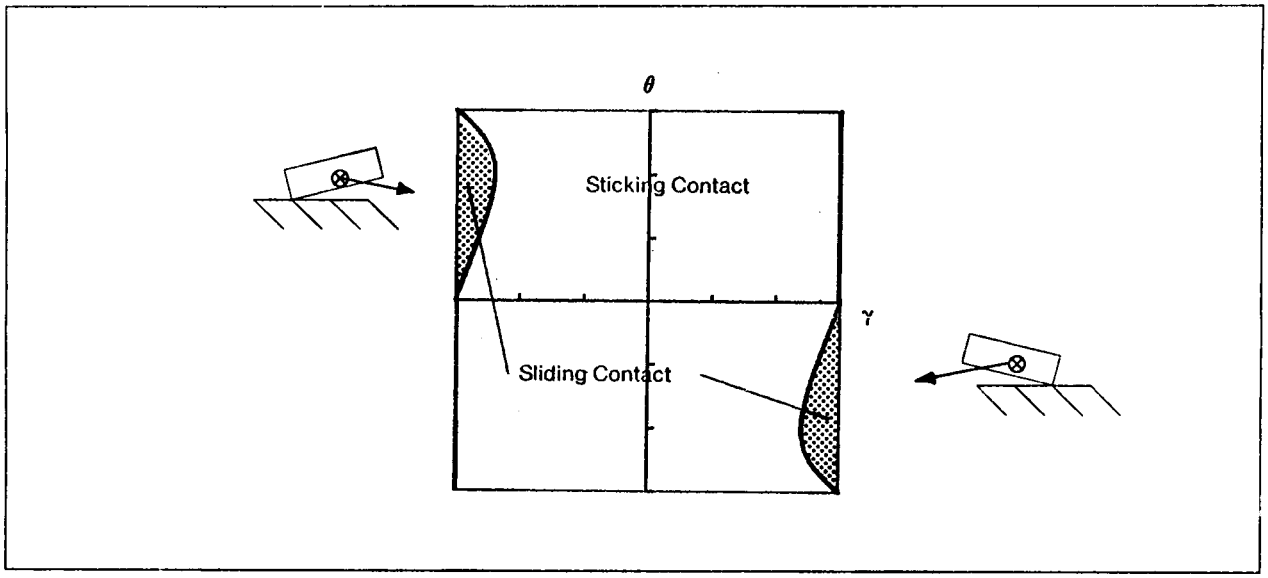


Figure 4.5. Impact with very large friction. The sliding contact occurs very large incident angles. In this example, $\alpha = 89.99$ degrees, $e = 0.8$, and $r = 1.414$.

5. Motions of Object after Impact

In this section we investigate the motion of an object after impact. The following questions are addressed:

1. How will the object rotate?
2. How does the local angle of reflected motion depend on the local angle of incident motion?
3. How do the answers to the above two questions differ from those obtained from the theory of elasticity?

These questions characterize the analysis of motions of the object and the outcome of various striking operations. The way that the object will rotate is referred as the fundamental motion of the object.

5.1. The Fundamental Motion

To qualitatively determine which way the object will change its rotating motion, we must determine the impulse generated in the process. From equation (3.1), the change of angular velocity of the object depends on where the impulse lies. If the impulse passes through the center of mass, then the right hand side of the third equation in equation (3.1) vanishes, and there is no change in angular velocity. If the impulse lies to the right of the center of mass, counter-clockwise change of rotation occurs, and if the impulse lies to the left of the center of mass, clockwise change of rotation occurs. We can represent the sense of change in rotation on the impact space diagram. The boundary between the clockwise and the counter-clockwise changes is where only the translational velocity change occurs. The boundary line splits the entire impact space into two regions as shown in Figure 5.1. This line is represented by a solid line and is called translation line.

In general, the traslation line consists of three segments lying in the sticking contact and the sliding contact regions. This is very similar to the traslation line of quasi-static process except that it is no longer an exact straight line. In quasi-static processes, it is a straight line with a 45 degrees slope angle (see [Brost 1986]). It is interesting to note that for a perfect plastic impact, i.e., $e = 0$, the translation line is identical to that derived from the quasi-static process. The segment of the line in the sticking contact region is a straight line with a slope angle of 45 degrees as shown in Figure 5.2. In other words, for a perfect plastic impact an object will turn the same way upon impact as it would in the quasi-static limit. On the other hand, a perfect elastic process produces another limit for the translation line. In general case, the translation line will lie in those regions bounded by the limits. These regions are shaded in Figure 5.2 and they represent the locus of the translation lines for all possible values of e.

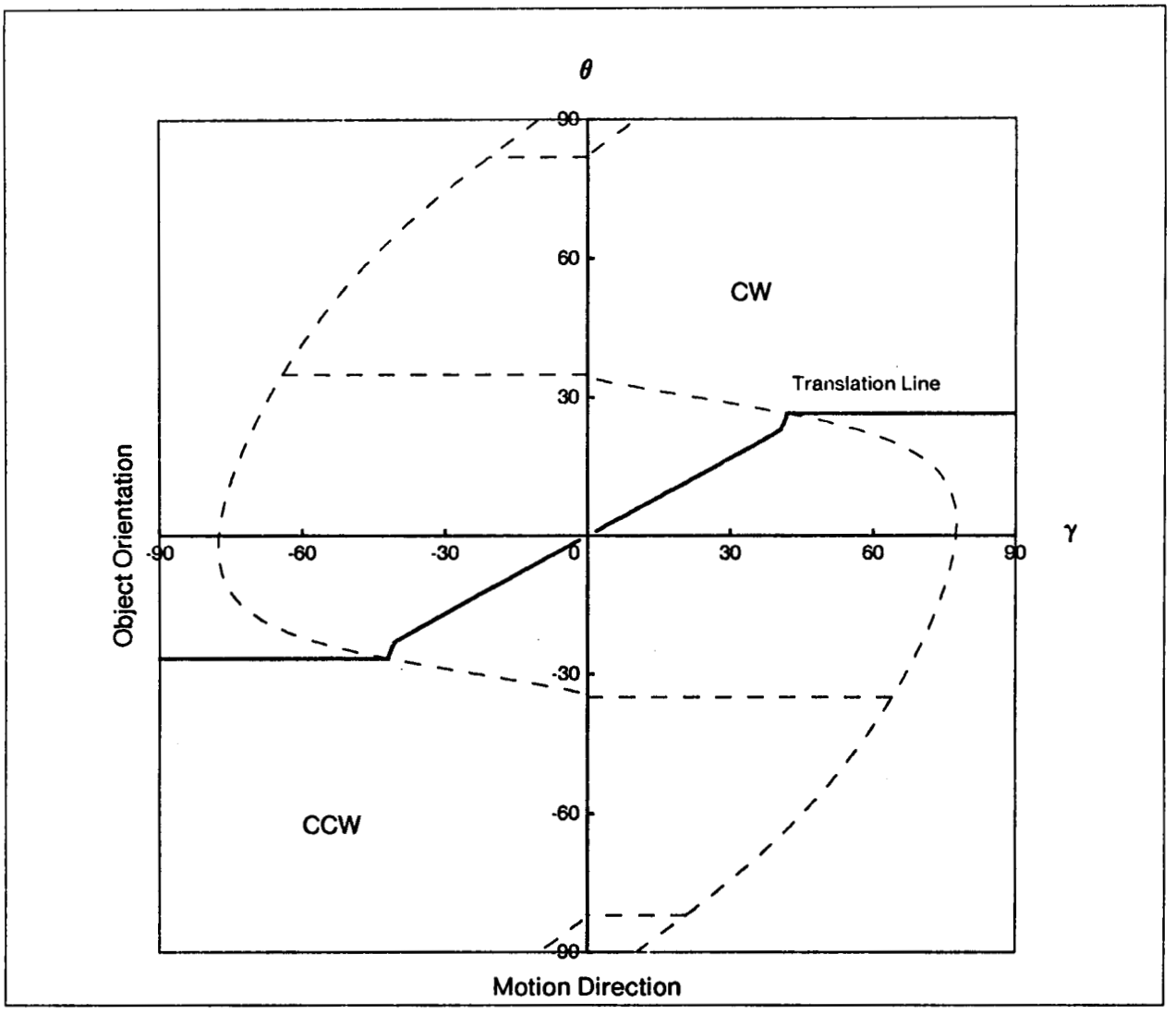


Figure 5.1. Changes in the rotational velocity at the point of contact. The solid line represent the boundary between the clockwise and the counter-clockwise changes. On this line, only a translational change of velocity occurs. In this example, $\mu = 0.5$, $e = 0.8$, and $r = 2$.

5.2. Local Velocity at the Point of Contact

Consider the rebound motion of the object at the point of contact. The normal rebound velocity v_{cy} is non-negative, while the tangential rebound velocity v_{cx} can be positive, negative, or zero, depending on the mode of contact happened in the process. Expressing the rebound motion by the rebound parameter $\tan\gamma_r = -v_{cx}/v_{cy}$, the rebound conditions are plotted in Figure 5.3. If the incident angle is large enough so that the sliding contact occurs, then the relations (3.11) and (3.13) are valid. Substituting these equations into equations (3.2) and (3.3), the governing relation of the incident parameter $\tan\gamma$ and

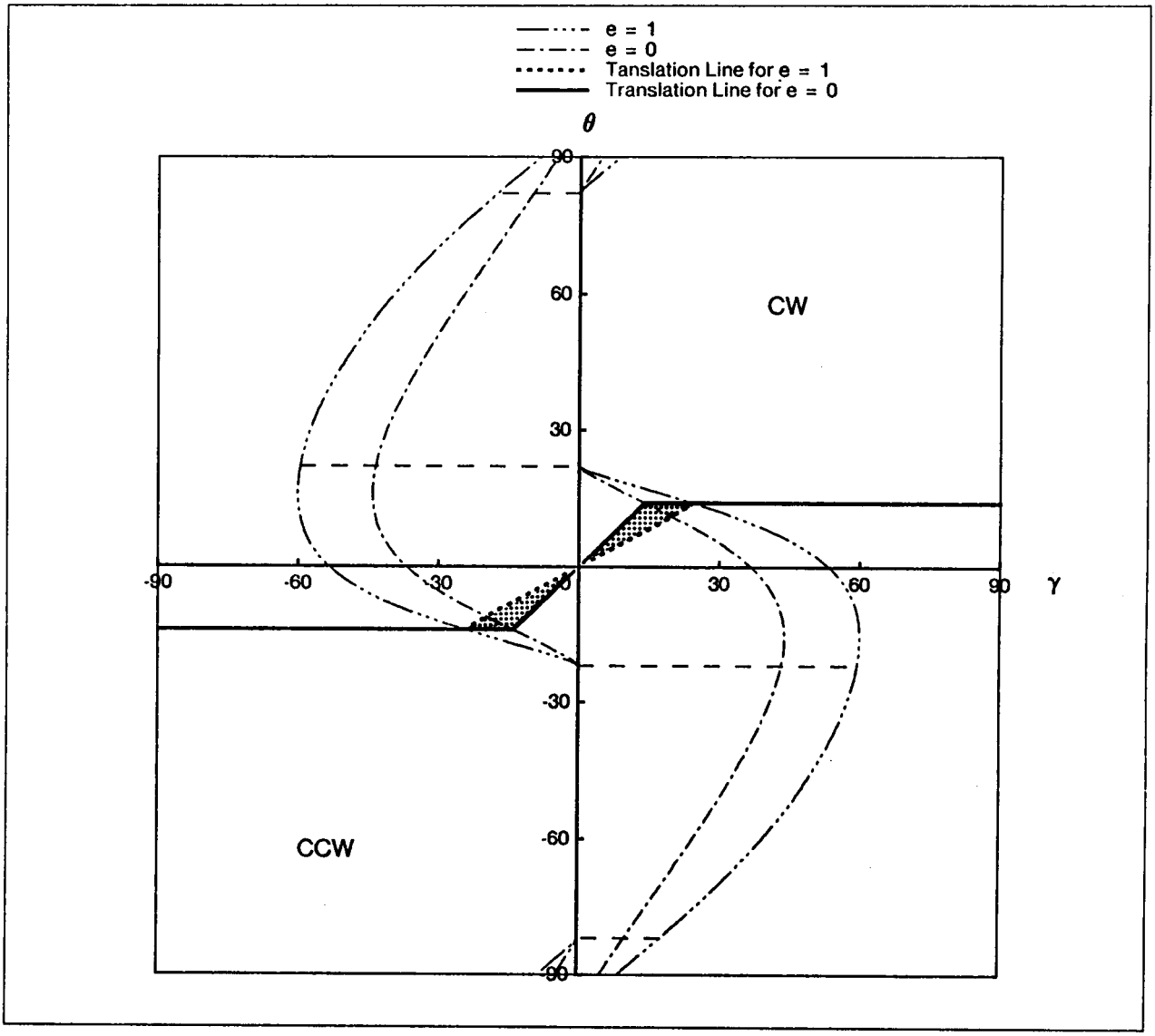


Figure 5.2. The locus of the translation lines for rotational velocity changes. $\mu = 0.25$, and $r = 1.414$.

the rebound parameter $\tan\gamma_r$ is given by:

$$e\tan\gamma_r = \tan\gamma + c \tag{5.1}$$

where c is a constant independent of the incident angle γ and is given as

$$c = (1+e)\frac{\mu[1+r^2+(\tan\theta)^2] - r^2\tan\theta}{\mu r^2\tan\theta - [1+r^2(\tan\theta)^2+(\tan\theta)^2]}. \tag{5.2}$$

If the sticking contact occurs, then the tangential rebound velocity is zero, corresponding to the conditions of rolling at rebound. When the reversed sliding contact occurs, negative angles of rebound can be obtained.

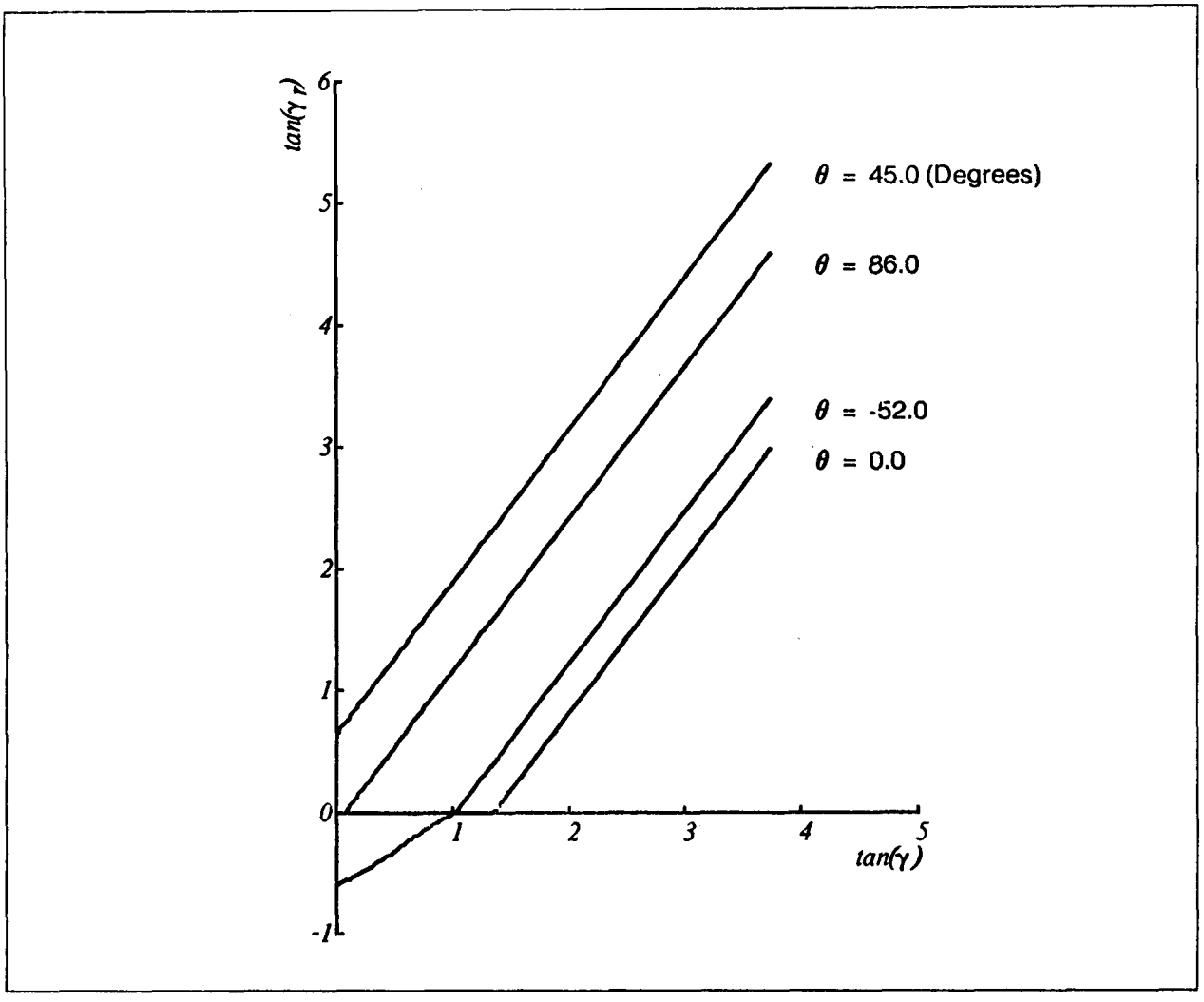


Figure 5.3. Rebound velocity at the point of contact. The rebound angle γ_r is a function of the angle of incidence γ. The parameters are given as $\mu = 0.25, e = 0.8$, and $r = 1.414$.

The rigid body theory agrees with the elastic contact theory for the impact of sliding contact (see [Maw, Barber, and Fawcett 1981]). The elastic theory takes into account contact deformation and frictional traction. It predicts that the tangential rebound velocity is negative when sticking contact occurs and the negative rebound is most likely to arise when the contact materials are easy deform, for example, rubbers. The simple rigid body theory presented in this paper, which ignores the contact deformation, predicts the zero tangential rebound velocity. However, for the eccentral impact problem, the simple theory gives a reasonable approximation to the contact modes and the motions of the object for all set of the geometric configurations of impact. For the rigid body model, the governing equations are a system of ordinary differential equations and the closed form solutions are obtained by means of Routh's graphic technique. With a more elaborate and perhaps more accurate elastic or elastic-plastic model, the system becomes more complex. It is perhaps difficult even to solve the problem numerically (see [Johnson 1985]).

6. Conclusion

In this paper, we represented all possible impacts by their geometric configurations. We defined an impact space that consists of all possible geometric descriptions. In this space, various modes of contact corresponding to the processes are found. For any given impact, we can predict how the direction of velocity of the point of contact varies.

The analysis incorporates friction, elasticity, and inertial property of an object. Within the model of the coefficient of restitution e, the loci found above are exact bounds on the translation lines of the object with an arbitrary elastic property. The bound corresponding to the lower value of e (perfect plastic, $e = 0$) is exactly what the quasi-static analysis predicts. The other bound corresponds to a perfect elastic impact ($e = 1$). Changes in friction and effective inertia produce large changes for contact regions and motions of the object.

The method used in this analysis can predict changes in the direction of sliding velocity. Calculating these changes is generally the main difficulty encountered by other theories. Therefore, within the domain of rigid body theory, our analysis can be applied to all possible impacts, whereas others can only be used in special cases.

We only discussed the qualitative change of rotation of an object in this paper. In general, the motion of the object can be represented by an instantaneous center of rotation (COR). Extending our analysis for the locus of CORs provides quantitative information of the object motion at impact. Loci for all possible impacts and all possible parameters are very useful for the understanding the inertia dominated motion. Furthermore, in all *real* robotic operations, a combination of impact dynamics (inertia dominated motion) and quasi-static dynamics (friction dominated motion) is involved. A comparison of the work of impact dynamics with previous work of quasi-static dynamics may make both work appliable to a broader range.

Other likely extensions of this research may include a full three-dimensional analysis of an impact and a development of the manipulator operations that employ the mechanics.

These research areas are currently under investigation in our CMU Manipulation Laboratory.

Acknowledgments

I would like thank Matt Mason for introducing me to the dynamic problem, and his valuable discussions and suggestions, and very useful comments on an early draft of this paper. I am most grateful to Randy Brost for his careful readings of drafts of this paper and his many comments and suggestions. I especially thank Michael Peshkin for his readings of the paper and suggestions on the extensions of the work. This research was supported by a grant from the System Development Foundation.

References

Beer, F.P, Johnston, Jr, E.R., Vector Mechanics for Engineers, Fourth Edition, McGraw-Hill, 1984.

Boothroyd, G., Redford, A.H., Poliand, C., Murch, L.E., Statistical Distributions of Natural Resting Aspects of Parts for Automatic Handling, *Manufacturing Engineering Transaction, Society of Manufacturing Automation,* Vol. 1, 1972.

Brach, R.M., Moments Between Impacting Rigid Bodies, *Transactions of ASME, Journal of Mechanical Design,* Vol. 103, pp. 812 - 817, October, 1981.

Brost, R.C., Automatic Grasping Planning in the Presence of Uncertainty, *IEEE International Conference on Robotics and Automation,* San Francisco, April, 1986.

Chelpanov, L.B., Kolpashnikov, S.N., Problems with Mechanics of Industrial Robot Grippers, *Mechanism and Machine Theory,* Vol. 18, No. 4, pp. 295–299, 1983.

Chumenko, V.N., Yushchenko, A.S., The Effect of a Blow on the Executive Mechanism of a Manipulational Robot, *Engineering Cybernetics,* Vol. 19, No. 4, 1981.

Drake, S.H., Using Compliance in lieu of Sensory Feedback for Automatic Assembly, Ph.D. thesis, MIT Department of Mechanical Engineering, September, 1977.

Erdmann, M.A., Mason, M.T., An Exploration of Sensorless Manipulation, *IEEE International Conference on Robotics and Automation,* San Fransisco, April, 1986.

Featherstone, R., Robot Dynamics Algorithms, Ph.D. thesis, Department of Artificial Intelligence, University of Edinburgh, 1984.

Goldsmith, W., Impact: The Theory and Physical Behavior of Colliding Solids, Edward Arnold Publishers Ltd., London, 1960.

Higuchi, T., Application of Electromagnetic Impulsive Force to Precise Positioning Tolls in Robot System, in *Proceedings of the Second International Symposium of Robotics Research,* Kyoto, Japan, August, 1984.

Hollerbach, J.M., Workshop on the Design and Control of Dexterous Hands, MIT Artificial Intelligence Laboratory A.I. Memo No. 661, April, 1982.

Johnson, K.L., Contact Mechanics, Cambridge University Press, New York, 1985.

Keller, J.B., Impact with Friction, *Journal of Applied Mechanics,* Vol. 53, pp. 1 - 4, March 1986.

Kilmister, C.W., Reeve, J.E., Rational Mechanics, American Elsevier Publishing Company, Inc., New York, 1966.

Mani, M., Wilson, W.R.D., A Programmable Orienting System for Flat Parts, NAMRI XIII Proceedings, University of California at Berkeley, May, 1985.

Mason, M.T., Manipulator Grasping and Pushing Operations, MIT Artificial Intelligence Laboratory , AI-TR-690, June, 1982.

Mason, M.T., The Mechanics of Manipulation, *IEEE International Conference on Robotics and Automation,* IEEE Computer Society, St. Louis, 1985.

Mason, M.T., On the Scope of Quasi-static Pushing, *Third International Symposium on Robotics Research,* Gouvieux, France, October, 1985.

Mason, M.T., Mechanics and Planning of Manipulator Pushing Operations, *International J. of Robotics Research,* Vol. 5, No. 3, 1986.

Mindlin, R.D., Deresiewicz, H., Elastic Spheres in Contact under Varying Oblique Forces, *ASME Journal of Applied Mechanics,* Vol. 75, pp. 327 – 344, 1953.

Maw, N., The Oblique Impact of Elastic Spheres, *Wear,* Vol. 38, pp. 101 – 114, 1976.

Maw, N., Barber, J.R., and Fawcett, J.N., The Role of Elastic Tangential Compliance in Oblique Impact, *Transactions of ASME, Journal of Lubrication Technology,* Vol. 103, pp. 74 – 80, 1981.

Parker, J.K., Paul, F.W., Characterization and Control of Object Acquisition with a Sensored Robot Hand, *American Control Conference,* San Diego, June, 1984.

Peshkin, M.A. and Sanderson, A.C., Manipulation of Sliding Object, *IEEE International Conference on Robotics and Automation*, San Francisco, California, April, 1986.

Routh, E.J., Dynamics of a System of Rigid Bodies, Macmillan and Company, Ltd., London, 1860.

Selvage, C.C., Assembly of Interference Fits by Impact and Constant Force Methods, M.S. Thesis, MIT Department of Mechanical Engineering, June, 1979.

Whitney, D.E., Force Feedback Control of Manipulator Fine Motions, *Journal of Dynamic Systems, Measurement, and Control*, pp. 91 – 97, June, 1977.

Whittaker, E. T., A Treatise on the Analytical Dynamics of Particles and Rigid Bodies, Cambridge, 1904.

Zheng, Y.F., and Hemami, H., Impact Effects of Biped Contact with the Environment, *IEEE Transactions on Systems, Man, and Cybernetics,* Vol. SMC - 14, No. 3, pp. 437 – 443, May/June, 1984.

Appendix A

In the general impact of two bodies the impulse forces exerted on the bodies are applied at A and B respectively. Let's consider the body to which the point A belongs. We denote the components of the normal, tangential, and rotational velocities of the center of mass at the moment of the greatest compression by V_n, V_t, and Ω, respectively. The components of the impulse in the period of compression are denoted by P_{nC} and P_{tC} (Figure A.1). In the common normal and tangent rectangular coordinate system, the equations of motion at the instance are given as:

$$\begin{aligned} mv_{no} - P_{nC} &= mV_n \\ mv_{to} - P_{tC} &= mV_t \\ m\rho^2\omega_o - aP_{nC} - bP_{tC} &= m\rho^2\Omega \end{aligned} \tag{A.1}$$

where a and b are the projections of the distance of the center of mass to the contact point on the common tangent and the common normal.

Similarly, for the period of restitution, we obtain

$$\begin{aligned} mV_n - P_{nR} &= mv_n \\ mV_t - P_{tR} &= mv_t \\ m\rho^2\Omega - aP_{nR} - bP_{tR} &= m\rho^2\omega \end{aligned} \tag{A.2}$$

where P_{nR} and P_{tR} are the components of the impulse in the period of restitution. From these equations, we can obtain the following relations:

$$\left.\begin{aligned} \frac{P_{nR}}{P_{nC}} &= \frac{V_n - v_n}{v_{no} - V_n} \\ \frac{P_{tR}}{P_{tC}} &= \frac{V_t - v_t}{v_{to} - V_t} \\ \frac{\Omega - \omega}{\omega_o - \Omega} &= \frac{aP_{nR} + bP_{tR}}{aP_{nC} + bP_{tC}} \end{aligned}\right\} \tag{A.3}$$

By the definition of the coefficient of restitution, we know that

$$\frac{P_{nR}}{P_{nC}} = e. \tag{A.4}$$

At this moment, let's assume that this relation also holds for the components of the impulse in the tangential direction, i.e.,

$$\frac{P_{tR}}{P_{tC}} = e. \tag{A.5}$$

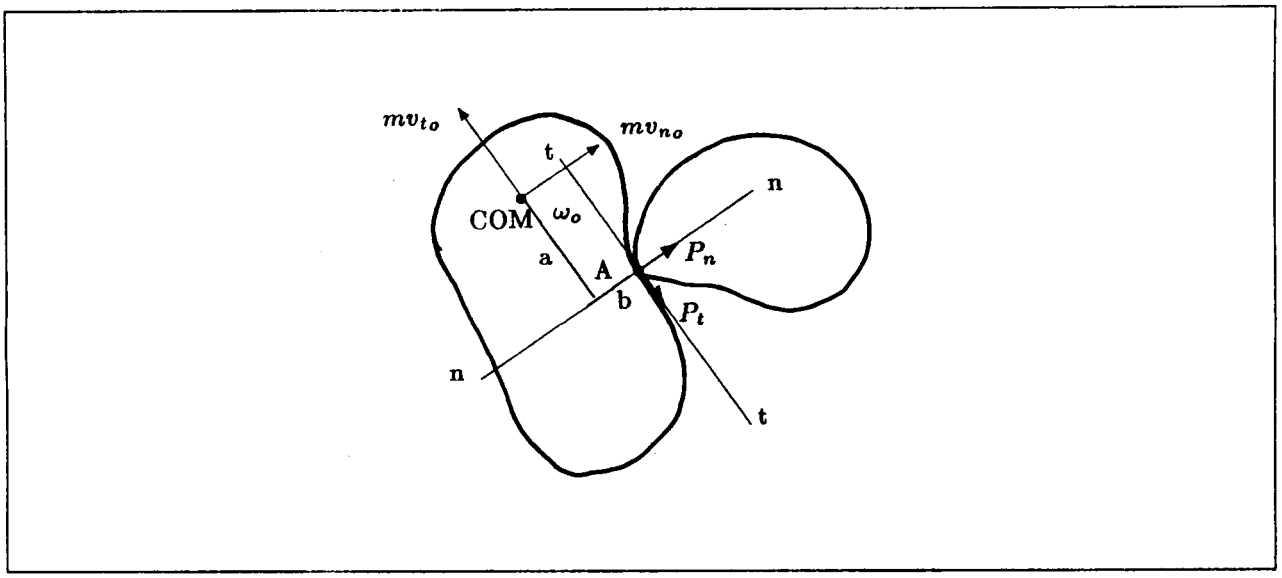


Figure A.1. General impact of two bodies. The initial components of the velocities of the center of mass of body A are v_{no}, v_{to}, and ω_o in the common normal and tnagetial coordinate system.

Then, we can show that the coefficient of restitution can be evaluated by the ratio of the relative normal velocities of the points in contact before and after impact. In other words, Poisson's hypothesis and Newton's law agree with each other under the assumption. We shall first prove the proposal, and then discuss the conditions under which equation (A.5) is valid.

Applying equation (A.3) to equations (A.4) and (A.5), the coefficient of restitution can be alternatively expressed as:

$$e = \frac{V_n - v_n}{v_{no} - V_n} \qquad e = \frac{V_t - v_t}{v_{to} - V_t} \qquad e = \frac{\Omega - \omega}{\omega_o - \Omega} \tag{A.6}$$

After a few manipulations, we have the following expression

$$e = \frac{V_n + a\Omega - (v_n + a\omega)}{v_{no} + a\omega_o - (V_n + a\Omega)} \tag{A.7}$$

This expression can be represented by the components of the velocity of the point of contact A as:

$$e = \frac{(V_A)_n - (v_A)_n}{(v_A)_{no} - (V_A)_n} \tag{A.8}$$

The analysis of the motion of the second body leads to a similar expression for e in terms of the components along the common normal of the velocities of point B. Noting that $(V_A)_n = (V_B)_n$, and eliminating these components, we obtain relation

$$e = -\frac{(v_B)_n - (v_A)_n}{(v_B)_{no} - (v_A)_{no}} \tag{A.9}$$

This relation is the expression of Newton's law. Therefore, it is equivalent to Poisson's hypothesis.

Now we discuss the conditions under which equation (A.5) is satisfied. In Section 3, the impact process analysis states that the representive point of the process will travel along either the line of limiting friction defined by equation (3.14) or the line of sticking. Both lines are linear in the impulse space (see Figure 3.2). If the impact is with the sliding contact, then the friction continues the limiting value throughout the process and discontinuity of friction dose not occurs. By the relation of equation (A.4) and a simple geometry in the impulse space, it is obvious that equation (A.5) is true. This provides us the first condition for the agreement of Poisson's method and Newton's method given in section 2.2.

For a direct impact, the tangent component of the relative velocity of the point in contact is zero. Then, $v_{cxo} = 0$ in equation (3.13), and the line of sticking crosses the origin of the impulse space. The representive point will travel at the beginning of the process and continue to travel along either the line of friction or the line of sticking. In both cases friction will never exhibit a discontinuity and equation (A.5) holds. This gives us the second condition for the agreement.